Master's Thesis
TVVR 19/5008

Modelling Water Exchange in the Flommen Lagoon, South Sweden

An investigation of physical processes and numerical modelling

Shuwei Wang

Division of Water Resources Engineering
Department of Building and Environmental Technology
Lund University

Modelling Water Exchange in the Flommen Lagoon, South Sweden

An investigation of physical processes and numerical modelling

By: Shuwei Wang
Supervisor: Professor Magnus Larson
Examiner: Professor Hans Hanson

Master Thesis

Division of Water Resources Engineering
Department of Building & Environmental Technology
Lund University
Box 118
221 00 Lund, Sweden

Water Resources Engineering
TVVR-19/5008
ISSN 1101-9824

Lund 2019
www.tvrl.lth.se

Master Thesis
Division of Water Resources Engineering
Department of Building & Environmental Technology
Lund University

English title:	<Modelling Water Exchange in the Flommen Lagoon, South Sweden>
Author(s):	<Shuwei Wang>
Supervisor:	<Magnus Larson>
Examiner:	<Hans Hanson>
Language	<English>
Year:	2019
Keywords:	<Water Exchange; Coastal Lagoon; The Flommen Lagoon; The Falsterbo Peninsula; Longshore sediment transport; Numerical modelling; Inlet morphology >

Acknowledgements

Here I sincerely give my appreciation to the doctoral student Almir Nunes De Brito Junior for all his help during this thesis project. During the first field measurement, I got the help from doctoral students Caroline Hallin and Clemens Klante which I appreciate a lot. I also want to give my thanks to Sebastian Bokhari Irminger, civil engineer at Sweco Environment AB, for providing the Degital Elevation Model and other information about the Flommen Lagoon.

A special thanks is given to my supervisor Professor Magnus Larson from whom I got this thesis opportunity. He has always been patient and giving great guidance and advices. His input and supervising motivated me to perform a better job during this project.

Abstract

The Flommen Lagoon in southern Sweden is surrounded by several natural reserves and is an important bird migration site on the edge of the continent. The protection of this area including water quality in the lagoon and flooding problems in the adjacent area has always been a concern.

The objective of this study is to simulate the water level in the Flommen Lagoon and the water exchange between the Flommen Lagoon and the sea with regards to inlet properties, longshore sediment transport and the operation of the sluice gate on the lagoon inlet to minimize the impact of human activities and reach a suitable operation strategy of the sluice gate. An investigation was also performed about the impact of constructing a second inlet between the lagoon and the sea.

According to the simulation results, the longshore sediment transport rate is larger in the south of the inlet than in the north which will result in sand accumulation around the inlet. The inlet geometry showed no significant influence on the lagoon water level but affected the water exchange rate. For the simulated time period, halve the cross-section area decreases the gross exchange rate by 39.2% and double cross-section area increases the gross exchange rate by 15.3%. The sluice decreases gross water exchange rate by 31.6%, but it plays an important role in protecting the golf courses around the lagoon from flooding. With two inlets, gross water exchange rate is 15.3% higher than with one inlet, and water level is also slighter higher.

Key words: Water exchange, Coastal lagoon, The Flommen Lagoon, The Falsterbo Peninsula, Longshore sediment transport, Numerical modelling, Inlet morphology

Table of contents

Acknowledgements iii
Abstract v
Table of contents vii
Introduction 1
Background 1
Objectives 3
Procedure 4
Physical processes in a coastal lagoon 5
Coastal lagoon 5
Water exchange in coastal lagoons 6
Renewal time 7
Inlet morphology and it's changes 7
Mathematical modelling of water exchange 9
Study area 12
General overview 12
Physical characteristics 12
Environmental functions 14
Economical values 15
Morphology 16
Climate 18
Precipitation 18
Temperature 18
Effect of climate change 19
Water level in the Skanör Harbour 21
Coastal processes at the Falsterbo Peninsula 22

Wind climate 22
Wave climate 23
Breaking waves 30
Longshore sediment transport 34
Water level in the lagoon 38
Field measurements 41
Setup and procedure 41
Lagoon morphology measurement 41
Lagoon water lever variation measurement 42
Data collection and analysis 43
Mathematical model 46
Assumptions 46
Governing equations 47
Case 1 47
Case 2 49
Case 3 49
Case 4 50
Numerical solutions 50
Explicit method 50
Semi-explicit method 53
Minimum area method 55
Water exchange and renewal time 55
Parameters and input 57
Calibration and validation 58
Simulation of different scenarios 63
Sinusoidal wave 63
Inlet geometry 65
Effect of the sluice gate 67

Water exchange rate 67
Extreme events 68
A second inlet 71
Conclusions 75
Reflection 76
References 77
Appendix 80
Calculation for sediment transport rate 80

Introduction

Background

Kjerfve (1994) defines a costal lagoon as *a shallow coastal water body separated from the ocean by a barrier, connected at least intermittently to the ocean by one or more restricted inlets, and usually oriented shore parallel*. Costal lagoons are usually very shallow with a water depth of a few metres. Costal lagoons are commonly found in all continents and consist of about 13% of the total shorelines around the world. As a result of the vital location of costal lagoons, they are usually of significant environmental and economical values. Water exchange in costal lagoons can be caused by several different factors such as river inflow, wind, tide, precipitation, surface runoff, groundwater infiltration and evaporation.

The Flommen Lagoon is located on the Falsterbo Peninsula in the Vellinge Municipality, Skåne province, which belongs to the southernmost part of Sweden (Figure 1 and Figure 2). The Falsterbo Peninsula is a densely populated area with about 200 inhabitants per square kilometer. As a famous bird migration site and marine nature reserve, this area is of major environmental importance. It also has substantial economic value with regards to buildings and infrastructure, and the area is well-known for its beautiful beaches and for having some of the most famous golf courses in Sweden; these latter features implies that the peninsula is of significant touristic value. All these factors make it important to preserve the natural environment and minimize the negative impact of human activities.

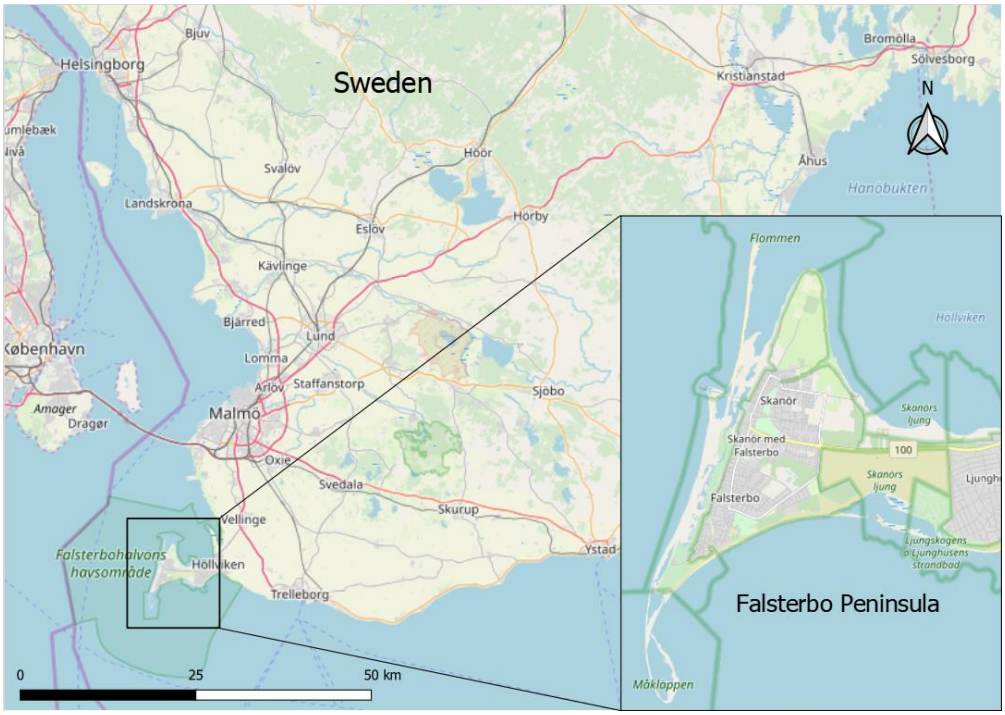

Figure 1. Location of the Falsterbo Peninsula.

Figure 2. Study area: the Flommen Lagoon along the west coast of the Falsterbo Peninsula.

Water discharged into the Flommen Lagoon from river and drainage is negligible. The water level in the sea together with the inlet channel and lagoon properties determine the water exchange between the lagoon and the sea, thus, the water quality in the lagoon. The Falsterbo Peninsula is a sandy deposit, implying that the coastal area is very dynamic and the morphology is highly changeable, which affects the inlet properties and the water exchange. The inlet morphology is controlled by both natural processes and human activities which include the costal sediment transport by waves and currents, the transport by the inlet exchange flow and regular dredging by the municipality. In order to ensure acceptable environmental conditions in the lagoon, it is crucial to estimate the water exchange, which includes the influence of sedimentation on inlet properties. A related aspect is flooding of the areas adjacent to the lagoon that is a potential problem for buildings and infrastructure. To remediate the flooding problem, a sluice gate was installed in the summer of 2016 to prevent inflow during high water levels in the sea; concerns have been raised that this gate has changed the sedimentation at the inlet, increased the tendency towards closure and reduced water exchange.

Objectives

The overall aim of the study is to investigate the water exchange between the lagoon and the sea using different scenarios. In order to achieve this aim, the work will include the following objectives:

- To understand the physical processes governing the water exchange at the Flommen lagoon, including the influence of inlet properties and how they are affected by the coastal sediment transport.

- To develop and apply a mathematical model for quantifying the water exchange under different conditions with focus on the influence of changes in the inlet properties.

- To assess the impact of the constructed gate on the water exchange and sedimentation at the inlet to arrive at suitable strategy to operate the gate.

- To simulate the impact of constructing another inlet on the on the water exchange.

Procedure

The study started with a comprehensive literature review about costal lagoon hydrodynamics, including lagoon water exchange and its mathematical modelling. Also, inlet morphological processes were studied including sediment transport along the coast and through the inlet. A comprehensive search was performed to locate available information about the study area around the Flommen Lagoon and compile existing data series of relevance. Background data encompasses bathymetric, topographic, geological, and meteorological conditions (e.g., such as wind speed and direction). Water level data from Skanör Harbour was compiled and analysed.

Two measuring campaigns were undertaken to determine the bathymetry of the lagoon and water levels at 5 locations in the lagoon simultaneously with the level in the harbour to be used for analysis and model calibration and validation since at present very limited information is available on this.

A mathematical model was developed to describe the response of the water level in the lagoon to changes in the sea level. The model was based on the classical work of Keulegan (1967). In his model, the lagoon was represented by a single basin having one representative water level and the surface area of this basin may vary with the water level to describe arbitrary bathymetries. In this report, as the lagoon is rather long and has a complex shape, it was divided into five small basins connected by channels with different frictional properties. Model parameters were selected following estimates from the literature. Calibration and validation of the model were performed with measurement data on water level variation in the lagoon.

The inlet morphological behaviour was studied by investigating the sediment transport along the coast and through the inlet channel. The former was calculated from the wave climate estimated based on a wind time series from Falsterbo using an enhanced SPM model. The derived wave climate was used to determine the longshore sediment transport.

The validated model was employed to simulate the water exchange for different scenarios with regard to the inlet characteristics, determined based on the inlet morphology and its change. The influence of the gate to control the water exchange was also investigated.

Physical processes in a coastal lagoon

In this chapter, general information and terminology, mechanism of water exchange in a coastal lagoon, lagoon inlet morphology and basic theory of mathematical modelling of water exchange will be introduced.

Coastal lagoon

As mentioned in the previous chapter, a coastal lagoon is a coastal water body which is usually oriented parallel to the coastline and only a few meters deep.

There is a common misunderstanding in the definition of estuary, fjord and coastal lagoon. In their paper, Kjerfve and Magill (1989) mentioned the differences between these inland water bodies. An estuary is affected by tides and drainage, usually with a depth not exceeded 20 m. A fjord is affected by tides and drainage, with a depth of several hundred meters. Water in fjords is usually stratified due to different salinity. A coastal lagoon may or may not be affected by tides (which means the salinity of lagoon water varies from each other), with a depth of only a few meters.

Kjerfve (1986) also divided costal lagoons into three systems with regards to geomorphology: chocked, restricted and leaky systems. Choked lagoons have only one long and narrow inlets connected to the ocean and commonly located in areas which are subject to high wave energy and strong longshore transport. The Flommen Lagoon is a typical example of chocked systems. Restricted systems have two or more inlets and usually show no vertical stratification. Leaky systems are usually of rather long and thin shape which have unlimited water exchange passes. They usually appear in areas where tide is dominated in littoral drift. Figure 3 shows the sketch of choked lagoon, restricted lagoon and leaky lagoon.

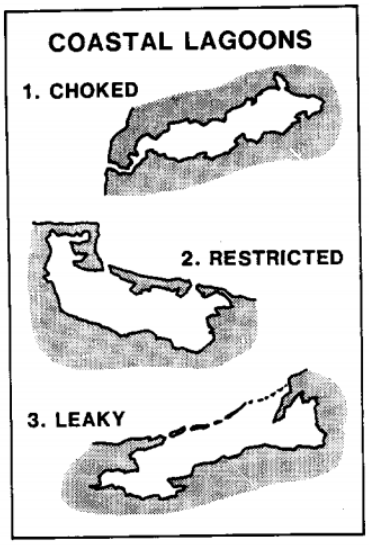

Figure 3. A sketch of three different types of coastal lagoons (Kjerfve and Magill, 1989).

Water exchange in coastal lagoons

Water exchange in coastal lagoons is a main factor that controls the water quality and physical conditions in the lagoon. Water exchange can be generated by different mechanisms which include tidal currents, wind generated circulation, wave currents, river discharge, surface runoff, groundwater and seawater influx and outflux and evaporation. The importance of these mechanisms varies in every lagoon and changes over time. In general, tidal currents and river inflow are the dominate factor in most coastal lagoon.

Tidal currents have more significant influence on restricted and leaky lagoons than on choked lagoons as the long narrow inlet has a "filter effect". When quantitatively analyzing the effect on water exchange from tidal currents, tidal prism (P) is usually used to describe the amount of water that is exchanged during a tidal cycle (O'Brien, 1931). It is defined by the following equation:

$$A = aP^m \quad (1)$$

where

A = cross section area of the inlet

a, m = coefficients determined by inlet conditions

River inflow is another important factor for water exchange and lagoon water quality. It decreases the lagoon water salinity and may cause stratification in the lagoon. River discharge is also the main source of nutrient and pernicious substances input, which is essential for the aquatic ecosystem.

Renewal time

The water quality in a lagoon is typically determined by the water exchange with the sea that occurs through the inlet. If there is negligible runoff from land, directly from surfaces or through some water courses, it is only water from the sea that can renew the lagoon water and improve the water quality. A wide range of parameters have been developed to quantify the water exchange and its characteristic time scales using terms such as “mixing”, “retention”, “renewal”, “residence”, and “flushing” time. Takeoka (1984) pointed out in his paper that the average residence time is the suitable time scale when studying water exchange problems. The commonly used definition for residence time is defined by Zimmerman (1976) as the time it takes for a certain particle to exit the lagoon from where it is. By applying advection-dispersion equation to a one-dimensional reservoir, the average residence time for a reservoir can be calculated.

The basic idea behind these concepts is to estimate the time it takes to replace the water volume in the lagoon regarding the exchange flow through the inlet. For the simple case of a single lagoon with one inlet the expression for the renewal time (T_R) is:

$$T_R = \frac{V}{Q} \tag{2}$$

where

V = the lagoon volume
Q = the exchange flow

Inlet morphology and it’s changes

Inlet is the passage between lagoon and the ocean through which water, aquatic creatures and other substance can be exchanged. It also serves as a navigable way for human to access the ocean and the bay when the lagoon is used as a harbor. As the continuous and effective substance exchange with

the ocean is very important to the lagoon ecosystem and sometimes economics, the inlet stability and morphology change is quite important.

Inlet morphology usually changes a lot over time. Inlet hydrodynamic conditions can be dependent only on ebb and flood tides or on the combined effect of wind stress, wind waves, tide and freshwater influx (Coastal Engineering Manual, 2012). There are different factors affecting inlet stability such as waves, tidal currents, deposition, inlet flow velocity and tidal conditions. When the shoreline is controlled by littoral transportation, if the flow away from the lagoon (ebb current) is not high enough, sediments will accumulate near the inlet and forms a sandy bar called spit and change the inlet size and geometry. While sediment is one factor affecting the inlet morphology, the influence of the local geological conditions is also as important.

Besides what has been discussed above, human activity also has a significant influence on the inlet morphology. As the inlet is vital for the ecological and economical functions of the lagoon, the inlet is usually dredged regularly.

The following figure shows the inlet morphology changes of the Flommen Lagoon. The spit around the inlet growth and disappearance happens during time. Also, before the sluice gate on the inlet was constructed in 2016, the inlet was manually closed sometimes by putting sand in the inlet to protect the lagoon from flooding. The picture from March 2013 is a result of this activity.

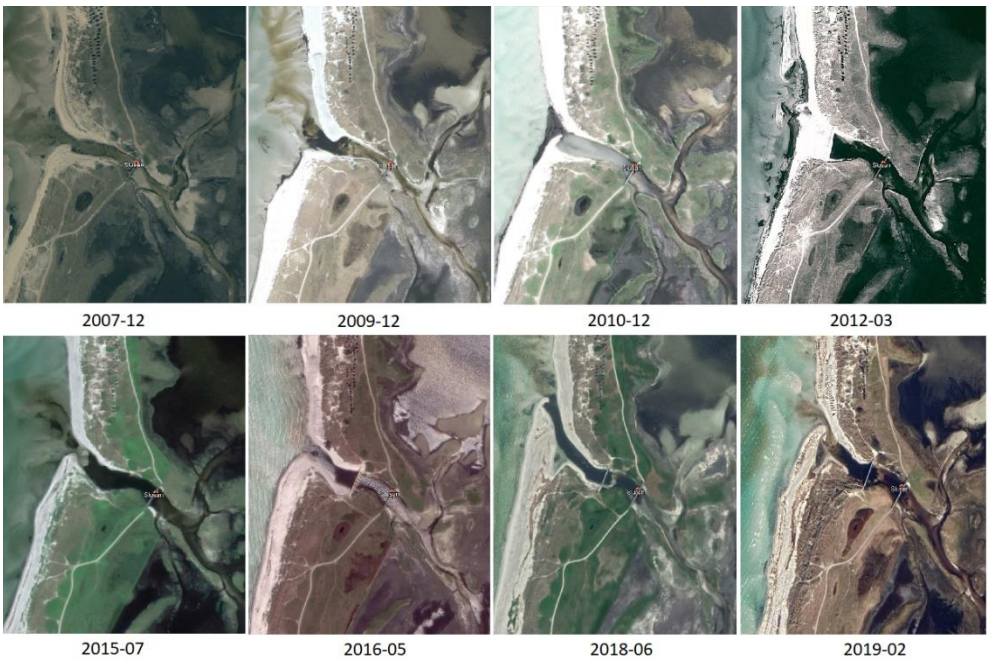

Figure 4. Morphology changes of the inlet of the Flommen Lagoon during 2007-2019. Source: Google Earth.

Mathematical modelling of water exchange

Keulegan (1967) introduced a simple mathematical model for water exchange in a lagoon. In this model, the whole lagoon is calculated as one box. Tidal currents and river inflow are the only factors that influence water exchange. The lagoon is assumed to be well-mixed and the water level in the entire lagoon is the same.

Water volume in the lagoon is controlled by water exchange between the sea and the lagoon and river inflow, so the water volume conservation equation is expressed as:

$$\frac{d(A_L h_L)}{dt} = Q_I - Q_R \tag{3}$$

where

t = time
A_L = Lagoon surface area
h_L = Lagoon water level

Q_I = water inflow through the inlet, $Q_I > 0$ for water flow into the lagoon and $Q_I < 0$ for water flow out from the lagoon
Q_R = river inflow

The momentum conservation equation between the sea and the lagoon can be expressed as:

$$h_0 = h_L + k_f \frac{u_I |u_I|}{2g} \tag{4}$$

where

h_0 = sea water level
h_L = lagoon water level
k_f = loss coefficient for the inlet
u_I = water velocity through the inlet, $u_I > 0$ for flow into the lagoon and $u_I < 0$ for water flow out from the lagoon
g = acceleration due to gravity

$$u_I = \frac{Q_I}{A_I} \tag{5}$$

where

A_I = inlet cross-section area

$$k_f = k_{en} + k_{ex} + \frac{f \cdot L}{4R} \tag{6}$$

where

k_{en} = entrance energy loss coefficient
k_{ex} = exit energy loss coefficient
f = Darcy - Weisbach friction term
L = inlet length
R = inlet hydraulic radius

$$f = \frac{116n^2}{R^{1/3}} \tag{7}$$

where

n = Manning's roughness coefficient

$$R = \frac{A_{avg}}{P} = \frac{A_I}{B + 2d} \tag{8}$$

where

P = Average wetted parameter

$B =$ width of the inlet
$d =$ depth of the inlet

Study area

General overview

Physical characteristics

The Flommen Lagoon is located between 55 ˚23’ to 55 ˚25’ North Latitude and 12 ˚49’ to 12 ˚50’ East Longitude. The Flommen Lagoon is elongated with a total length of approximately 3 km and a total area of 560 hectares.

In the northwest part of the lagoon, there is one opening connecting the lagoon to the sea (Figure 5). There is a sluice gate on the inlet channel since 2016 (Figure 6). The lowest level of this gate is -0.35 m, meaning that when sea water level is below -0.35 m there is no inflow from the sea. And the gate is manually closed when sea level is above 0.5 m, which means no water exchange between the lagoon and the sea when sea level is above 0.5m.

Figure 5. Location of the inlet. Source: Google Earth.

Figure 6. The sluice gate on the inlet. Photo by: Shuwei Wang.

No river flow and negligible drainage water are discharged into the lagoon. According to Swedish Meteorological and Hydrological Institute (SMHI, 2019), the highest hourly rainfall in Falsterbo was 9.9 mm/hour in 2010 to 2018, which can also be neglected. Therefore, the main water exchange is with the sea through the inlet. However, according to a report from Sweco (2019), the salinity of lagoon water is slightly lower than seawater, especially in the southern part of the lagoon (Figure 7 and 8). This indicates that groundwater infiltration also has some influence on the water quality in the lagoon. The influence of groundwater infiltration is not discussed in this report due to the lack of available data.

Figure 7. Chloride concentration measurement points. Source: Google Earth, Sweco (2019).

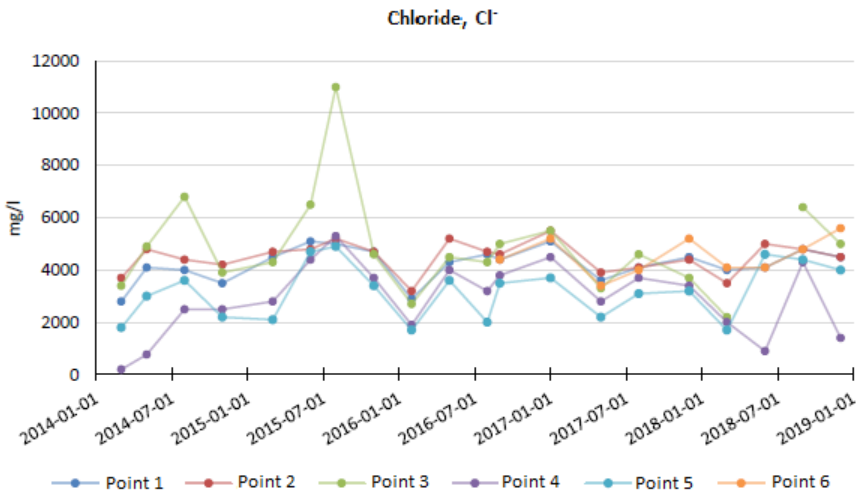

Figure 8. Chloride concentration at different location in 2014 to 2019 (SWECO, 2019)

The normal tidal range in the adjacent Baltic Sea is typically less than 0.25 m (Hanson, 2007), so the influence of tide in this area is small; instead it is the large-scale water movement in the Baltic Sea that determines the water level variation outside the Falsterbo Peninsula.

Environmental functions

The Falsterbo Peninsula is famous as a bird migration site. According to the 2017 annual report from Falsterbo Bird station, the total number of birds tracked in the peninsula was 16,788 of 103 species in 2017. The total number of birds marked at the station from 1947 to 2017 is 1,177,286 of 229 species (plus 4 kinds of hybrids).

Apart from the consideration for birds, there are also several natural reserves in the peninsula to protect habitats, vegetations and creatures. The whole Flommen Lagoon is included in the Flommen Natural Reserve. Some species in this reserve are categorized as vulnerable (sternula albifrons, a seabird; natterjack toad), highly threatened (Eryngium maritimum, a costal plant) and actually threatened (European green toad) by the Swedish Red List (Rödlistning).

Figure 9. One common vegetation around the Flommen Lagoon. Photo by: Shuwei Wang.

Economical values

The major economic value of Falsterbo Peninsula lies in recreation and tourism. The main industry of Falsterbo is the large fishing pier at the port of Skanör. There is no agriculture land on the peninsula.

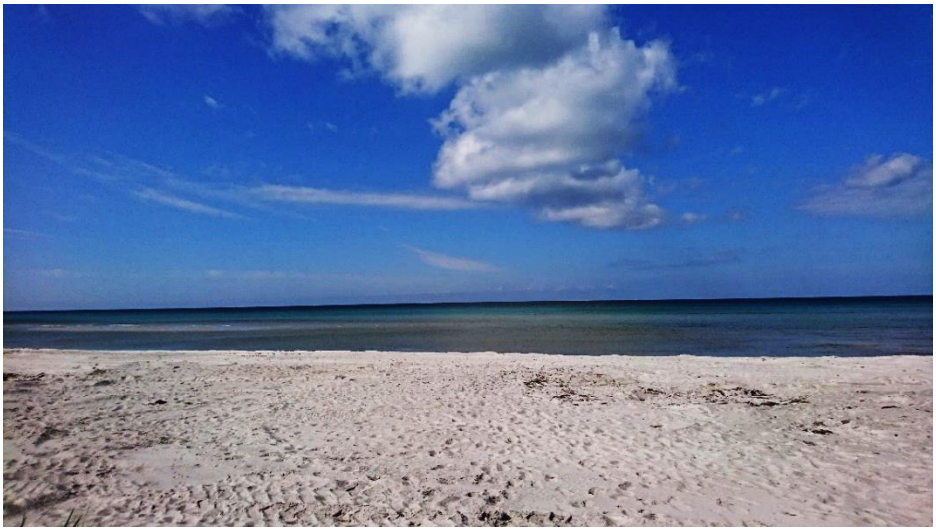

Figure 10. Beautiful sandy beach of the Falsterbo Peninsula. Photo by: Shuwei Wang.

As a famous bird observation site, Falsterbo Peninsula attracts more than 5000 birdwatchers every year. Meanwhile, the beautiful white sandy beaches, the annual Falsterbo Horse Show and two of the Swedish most famous golf courses also have significant tourist attractions and make Falsterbo a good recreation site and a popular summer vacation destination.

Figure 11. Swans swimming in a channel of the Flommen lagoon.

Morphology

As Nelson (1923) described in his article, the Falsterbo Peninsula is formed by the combined effort of costal currents and current drifts. Davidsson (1963) indicated in his book that the greater part of the peninsula is generated and developed during the post glacial time. As an example of "complex tombolo", this peninsula was formed by three different moraine kernels jointing each other: Ljunghusen (the middle part of the peninsula), Knösen (the northern part) and Falsterbo reef with Måkläppen island (the southern part) (Richeter,1936, cited in Davidsson, 1963).

The coastline of Falsterbo Peninsula is very dynamic and has experienced very noticeable morphological changes both in historic times and during the last few decades, especially the west and south coasts. This part of the coast is covered by sandy beaches which are of higher economical value but subject to stronger incoming wave energy. However, the north coast mainly

consists of vegetation and marshes and receives less wave energy; therefore, it experiences less erosion.

Hanson and Larson (1993) applied a numerical model to examine the net longshore sediment transport rate in the Falsterbo Peninsula. They got the results that an average net longshore transport rate along the west coast was of 35,000 m^3/year to the north and 61,000 m^3/year alone the south coast to the west. This also explains why the Måkläppen island has been experienced significant increase of its size. Figure 12 shows the morphological changes of the Måkläppen island in 60 years. According to Blomgren and Hanson (2000), this peninsula has not yet reached a final "equilibrium state" of its coastline.

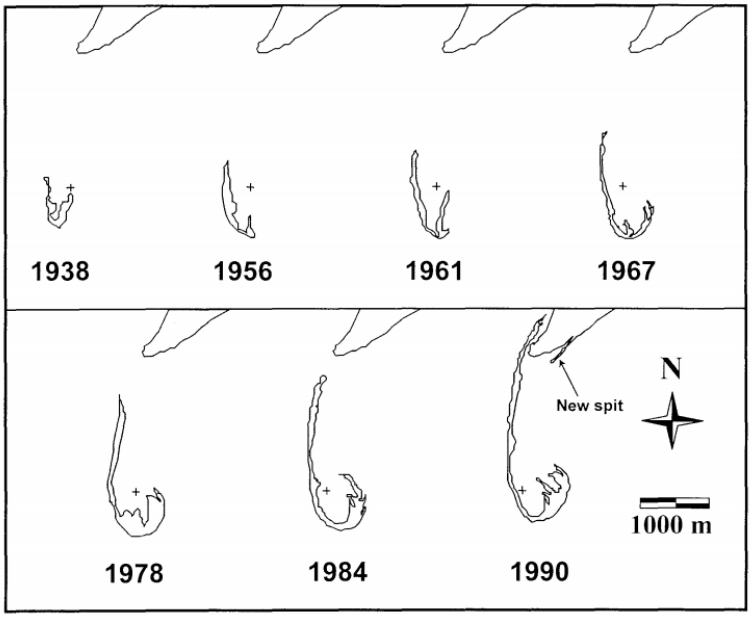

Figure 12. The morphological changes of the Måkläppen island, from 1938 to 1990 (Blomgren & Hanson, 2000).

Another factor that contributes to the morphological changes in Falsterbo Peninsula is the Skanör Harbour. After the construction of the Skanör Harbour in 1860, a downdrift spit was formed to the north of the harbour and keeps growing. As is shown in Figure 13, a significant and continuous growth of the spit was observed.

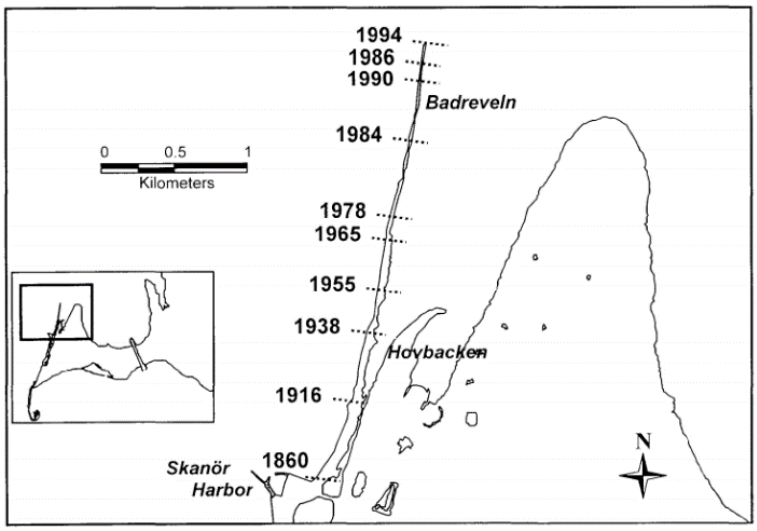

Figure 13. The morphological changes of the spit Badreveln (Blomgren & Hanson, 2000).

Climate

The Flommen Lagoon lays in southern Skåne county. This area experiences a relatively temperate climate. Four seasons here are distinct and temperature is rather mild through a year. The dominate climate in the Skåne county is marine climate. It is worth noting that due to the combined effect of the Gulf stream of the Bothnia and west wind drift, this area is warmer and drier than other regions at the same latitude.

Precipitation

The annual average precipitation in Skåne during 1961 to 1990 was 748 mm. The average of the year's maximum daily precipitation in Skåne county from 1961 to 1990 is 30 mm, but the amount varies in different years (from 20 mm to 55 mm) (SMHI, 2015). An increase of maximum daily rainfall was observed during 1991 to 2013.

Temperature

According to SMHI (2015), the annual average temperature of the Falsterbo Peninsula is 8 ℃. The winter average temperature of Skåne county was -0.6 ℃ during the reference period 1961-1990. Over the past 23 years, the winters have become somewhat milder in southern and inner Skåne. The summer average temperature during 1961-1990 was 15.4 ℃. The temperature is

evenly distributed over the county and rose slightly during the period 1991-2013.

Effect of climate change

Climate change will severely affect the Falsterbo Peninsula as the peninsula is very low-lying and its sandy beach is of great economic value and prone to flooding and erosion.

According to SMHI (2015), the temperature in Skåne continues to rise and by the end of the century, the temperature according to RCP 4.5 will rise by almost 3 degrees, while RCP 8.5 shows a 5-degree temperature increase.

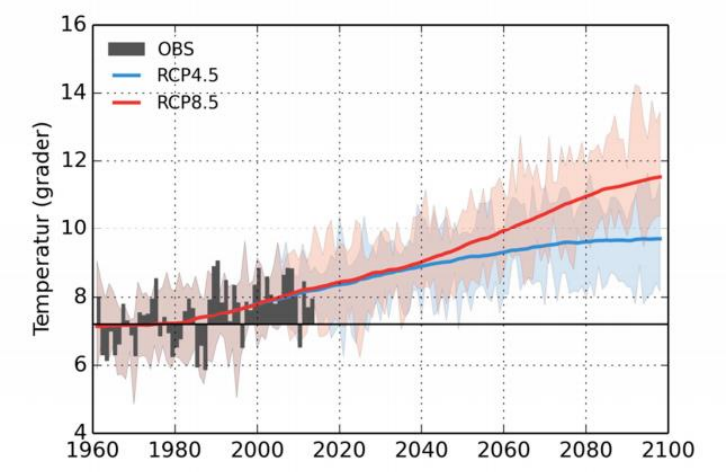

Figure 14. Temperature rise in Skåne county. Source: SMHI (2015).

The average global sea level rise between 1901 to 2010 is 0.91 m (IPCC AR5). Average sea level rise in Sweden based on observation from 14 measuring stations between 1886 to 2015 is shown as Figure 15. A similar trend as global sea level rise can be found in this figure.

Figure 16 shows the prediction of sea level in Falsterbo Peninsular in 2100 using RCP 4.5 and RCP 8.5. A large part of the Måkläppen Island, part of the beach and north of the Skanör Harbour will be flooded.

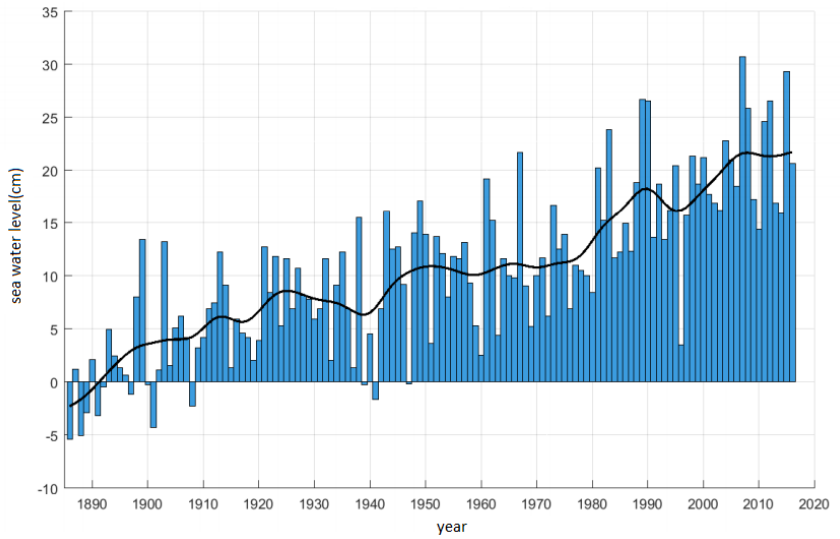

Figure 15. Net sea level rise in Sweden in 1886-2016 based on 14 Swedish sea level measuring stations. Source: SMHI (2017).

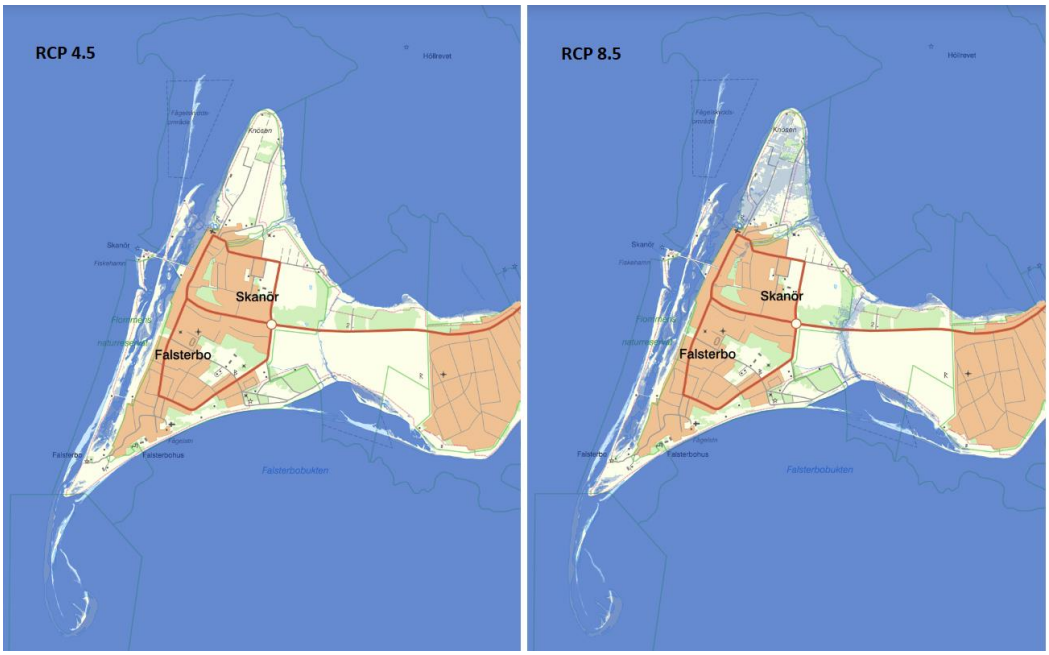

Figure 16. Sea level prediction in 2100 according to RCP 4.5 and RCP 8.5. This figure is generated by SGI from SMHI.

Water level in the Skanör Harbour

The sea level variation in the adjacent sea is measured hourly at the Skanör Harbour by SMHI. The sea level data is presented according to RH2000 height system with measuring date and time. This data series records sea level variations since 17th February 1992. In the data series, there are three levels for the data quality: controlled and approved values, suspected or aggregated values and uncontrolled values. The latest three months are not quality controlled. The location of the measurement station is shown below.

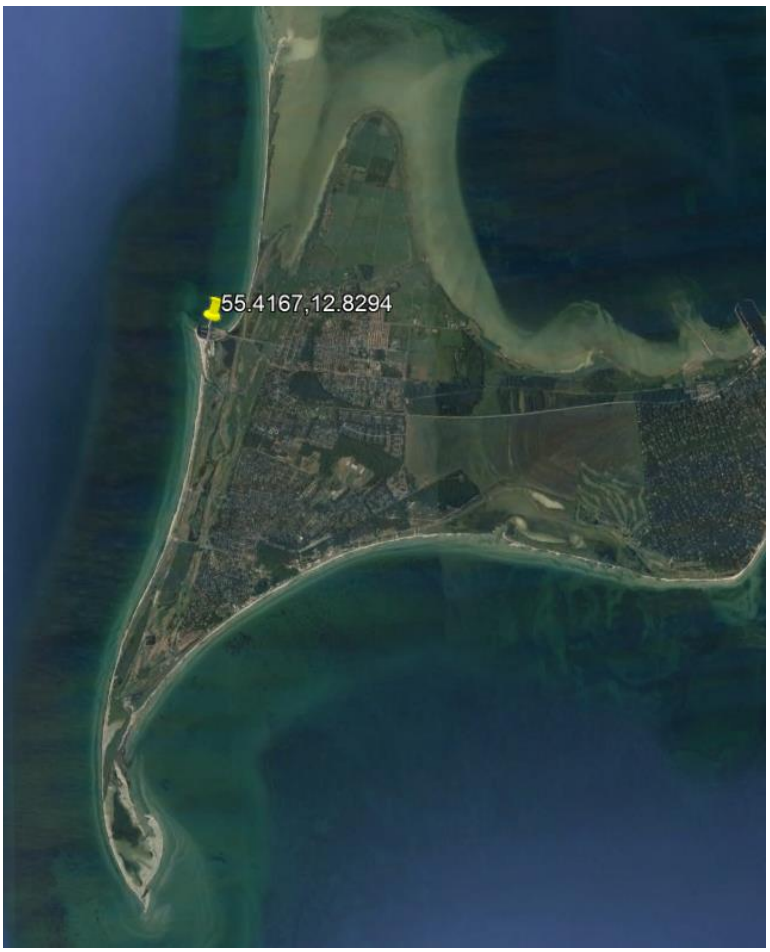

Figure 17. Location of the sea level measuring site at Skanör Harbour. Coordinate: 55.4146, 12.8294. Source: Google Earth.

Coastal processes at the Falsterbo Peninsula

Wind climate

Sweden is located in the westerlies, meaning that the prevailing wind is blowing from west or southwest. So is it in the Falsterbo Peninsula. Wind data used in this report was measured by SMHI. The anemometer site is located on the southwest corner of the peninsula (Figure 18). Due to no wind disturbance on the ocean and in the adjacent area, wind here is generally stronger than in the inland areas. The average wind speed at this station was 6.8 m/s during the period from mid-2009 to 2013.

Figure 18. Location of the wind measurement site. Coordinate: 55.3836, 12.8203. Source: Google Earth.

The wind rose showing the prevailing wind direction and windspeed distribution in Falsterbo is generated based on the 35-year wind observation data from SMHI. This data series consists of wind direction and windspeed

data based on average value of 10 minutes in every three hours from 1974 to 2009. The wind data was measured at 10 m above the ground. The maximum windspeed is 27 m/s. The average windspeed is 6.6 m/s.

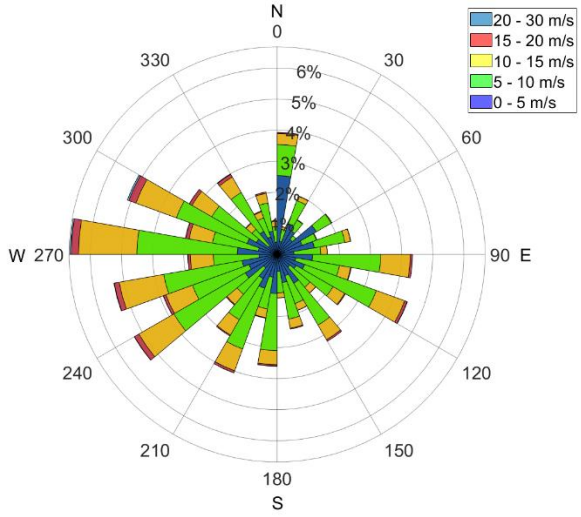

Figure 19. Wind rose of measurements in Falsterbo, based on wind data from 1974-2009.

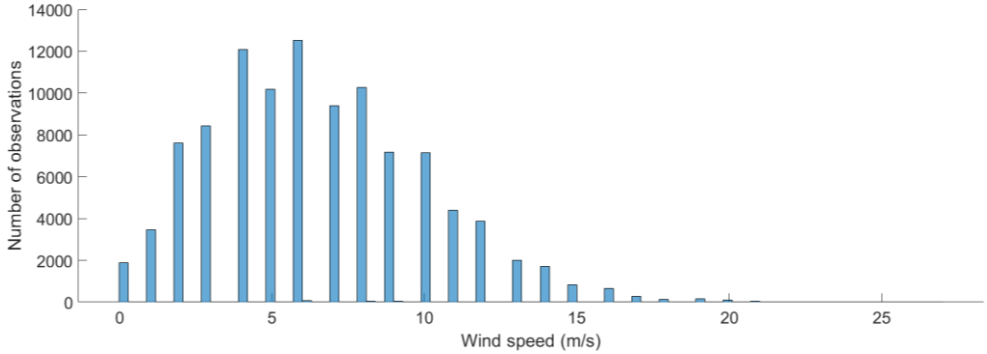

Figure 20. Histogram of wind speed in Falsterbo, based on measurement from 1974-2009.

Wave climate

Wave climate is defined as the seasonal and annual distribution of wave height, period and direction (CEM, 2002). It is a term commonly used to describe the climate over the sea. Wave climate is principally influenced by

wind climate at the same location, water depth and fetch length (Blomgren, et.al, 1999).

Hanson (2007) described the wave climate in the Falsterbo Peninsula as moderate as the average wave height is between 0 to 1 m. The ascendant wave direction here is western to southwestern.

When computing wind generated waves, wind data needs to be adjusted because below some thousand meters above surface, wind speed and direction is influenced by surface roughness, the elevation from mean surface, the temperature difference between the atmosphere and the ocean (SPM, 1984, p. 3-24). Also, sometimes wind data is measured onshore, not above the sea. Therefore, the wind data needs to be adjusted according to the elevation of the anemometer, the anemometer site's location, air-sea temperature difference and observation duration (if the windspeed is measured for less than 2 minutes).

The wind data is measured at the 10 m above ground. According to SPM (1984), it does not need elevation correction. The anemometer site in Falsterbo is located very close to the shore (about 300 m from the nearest shoreline), and there is no wind barrier in the adjacent area. Therefore, no location adjustment is needed. Due to lack of sea temperature data, the sea temperature is assumed to be the same as the air temperature which means the boundary layer has neutral stability and no temperature adjustment is needed. The windspeed data from the Falsterbo station is 10-minute duration-averaged, thus no duration correction is needed.

Furthermore, the windspeed used to predict wave conditions in SPM (1984) is the wind stressed factor U_A (also called the adjusted windspeed), the windspeed data (U, in m/s) from SMHI is therefore converted to wind stress factor by the following formula:

$$U_A = 0.71U^{1.23} \tag{9}$$

This windspeed is considered as a relatively constant average speed over the wind field (SPM, 1984). The wave climate near Falsterbo is then calculated from the adjusted windspeed U_A. A similar method is used here as in the report from Emanuelsson and Mirchi (2007).

When estimating waves, there are two conditions that can be calculated: fetch-limited and duration-limited. Fetch-limited condition is where the wave height has reached an equilibrium condition at the end of the fetch because the wind has blown constantly and long enough (SPM, 1984). Whereas duration-limited condition is where the wave height has not reached its equilibrium because the wind has not blown long enough. Different equations are applied for different conditions. In order to determine the condition under which the waves are, the spectral wave height H_{m_0} (in meters) and peak spectral period T_m (in seconds) are calculated.

In deep water (where water depth to wavelength *d/L* is larger than 0.5), the wave characteristics are independent of water depth (SPM, page 2-9). First, assume the waves are under fetch-limited condition. The spectral wave height H_{m_0} and peak spectral period T_m can be calculated if U_A and fetch length F (in meters) are provided:

$$H_{m_0} = 5.112 \cdot 10^{-4} U_A F^{1/2}$$

(10)

$$T_m = 6.238 \cdot 10^{-2} \left(U_A F\right)^{1/3}$$

(11)

$$t_m = 32.15 \left(\frac{F}{U_A} \right)^{1/3} \qquad (12)$$

where

t_m = the duation for fetch-limited condition (in seconds)

The fetch length is obtained by manually measuring the length from the inlet of the Flommen lagoon till another shore in different direction on map (see Figure 21). Values of fetch length and representative water depth in different directions are given in Table 1.

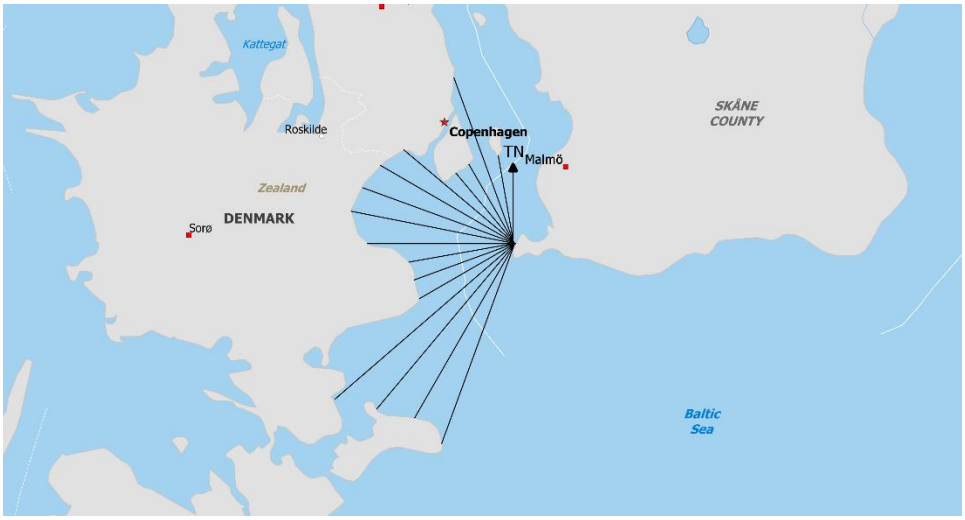

Figure 21. Fetch length measurement in different directions of the west coast of the Falsterbo Peninsular for wave condition calculation, measured every 10 degree. Directions in which wind does not generate waves are not included.

Table 1. Fetch length and representative water depth in different directions for wave condition calculation (true north: 0 degree).

Direction(degree)	Fetch length (km)	Representative water depth(m)
200	50	20
210	49	17
220	53	16
230	50	15
240	28	15
250	25	15
260	26	16
270	24	14
280	39	13
290	40	12
300	48	11
310	34	9
320	20	10
330	21	11
340	24	12

Eq. 10-12 are valid until the fully developed wave condition happens. So, the following equations are needed to check if the wave height and period exceed the fully developed wave condition (units are the same as in Eq. 10-12):

$$H_{m_0} = 2.482 \cdot 10^{-2} {U_A}^2 \tag{13}$$

$$T_m = 0.83 U_A \tag{14}$$

$$t_f = 7.296 \cdot 10^3 U_A \tag{15}$$

where

t_f = the duration needed for fully developed condition

If the actual wind duration t is longer than t_m, the wave condition is fetch-limited. Otherwise it is duration-limited. In this case, first the actual wind duration t should be used as t_m in Eq. 12 to calculate the equivalent fetch length. Afterwards Eq. 10 and Eq. 11 are used to calculate the spectral wave height H_{m_0} and peak spectral period T_m.

In shallow water where wave characteristics are affected by water depth, due to the bottom friction and percolation, the same wind and fetch conditions will generate waves with shorter period and smaller height than in deep water. The method for determining wave conditions is based on the method used for deep water in combination with wave energy theory. The following equations are used to determine the wave condition (notation as before):

$$\frac{g H_{m_0}}{{U_A}^2} = 0.283 \tanh\left(K_1\right) \tanh\left(\frac{K_2}{\tanh\left(K_1\right)}\right) \tag{16}$$

$$\frac{g T_m}{U_A} = 7.54 \tanh\left(K_3\right) \tanh\left(\frac{K_4}{\tanh\left(K_3\right)}\right) \tag{17}$$

$$K_1 = 0.53 \left(\frac{g d}{U_A^2}\right)^{3/4} \tag{18}$$

$$K_2 = 0.565 \left(\frac{g F}{U_A^2}\right)^{1/2} \tag{19}$$

$$K_3 = 0.833 \left(\frac{g d}{U_A^2}\right)^{3/8} \tag{20}$$

$$K_4 = 0.0379\left(\frac{gF}{U_A^2}\right)^{1/3} \tag{21}$$

$$\frac{gt_m}{U_A} = 537\left(\frac{gT_m}{U_A}\right)^{7/3} \tag{22}$$

The calculation for wave climate was done by Fortran code encompass with Eq. 10-22. A numerical approach based on the work of Dahlerus and Egermayer (2005) was employed in the code to calculate the wave condition for every timestep with regard to the wave revolution time.

$$\frac{dH}{dt} = \varphi\left(H_{eq} - H_{in}\right) \tag{23}$$

where

H = wave height
H_{eq} = new equilibrium height
H_{in} = wave height of the previous timestep
φ = a constant

$$H = H_{eq} - \left(H_{eq} - H_{in}\right)e^{-\mu\frac{t}{t_{\lim}}} \tag{24}$$

where

t_{lim} = the limiting duration, equals to tm
t = duration of the wind measurement
μ = a constant determined by a least-square fit method to the SPM wave growth function

The wave period is calculated by equations with the same manner as Eq. 23 and Eq. 24.

In this approach, if wind changes from a direction in which waves can be generated to a direction in which waves cannot be generated, waves will continuously decrease to zero in the same direction, until another wave can be generated.

The fetch length and representative water depth in Table 1 and wind stress factor calculated by Eq. 9 were used as input data in the Fortran code. The computed wave climate is plotted as a wave rose showing significant wave height and wave direction (Figure 22).

From the wave rose, the prevailing wave direction is from south-southwest, which comprises about 12% of all waves. The average wave height is 0.5663 m of all waves with non-zero height, which is consistent with the range of 0 to 1 m as described by Hanson (2007). The maximum wave height 2.86 m.

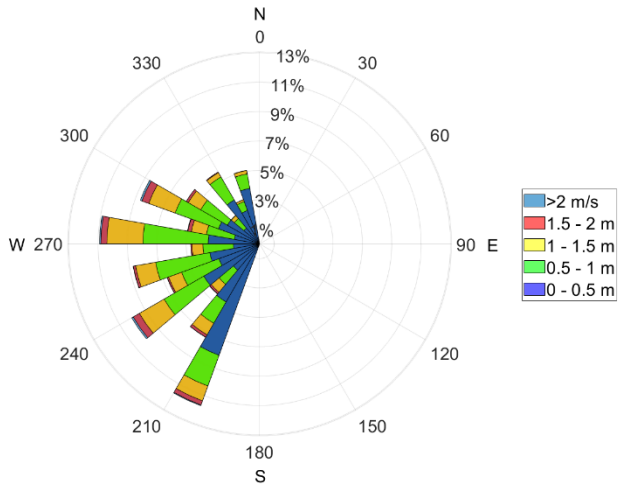

Figure 22. Wave rose generated from computed wave climate (of all waves with non-zero height).

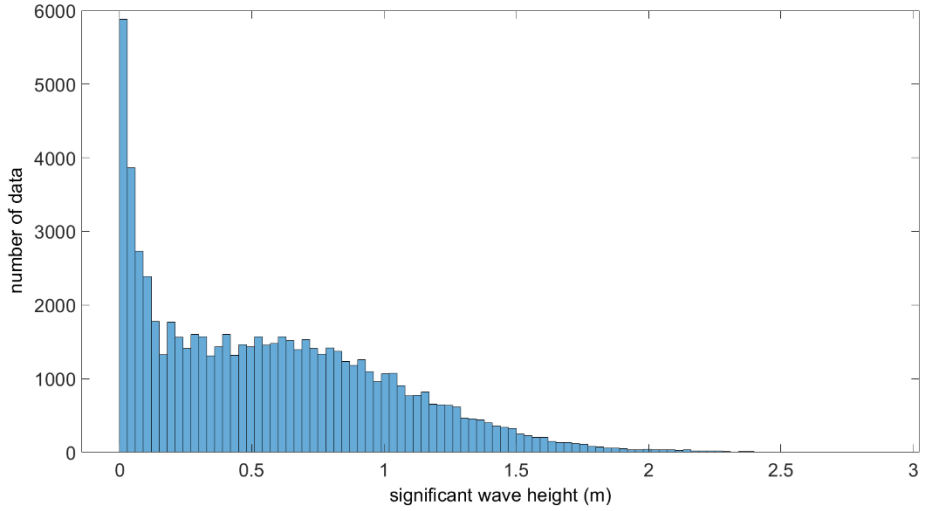

Figure 23. Wave histogram generated with computed wave climate (of all waves with non-zero height).

Breaking waves

Longshore currents along the coast of Falsterbo Peninsula is mainly generated by waves (Hanson 2007). Most sediment transport happens when waves break and generate longshore currents. When wave steepness reaches its maximum value for which waveform can remain stable, waves start to break. This is controlled by the following criteria:

$$H_b = 0.78\, h_b \tag{25}$$

where H_b and h_b are the wave height and water depth at breaking.

In this section, the computation of breaking wave height and angle is introduced as they are required for the computation of longshore sediment transport.

Wave energy flux per unit wavelength is given by:

$$P = EC_g \cos\alpha \tag{26}$$

And the total energy per unit crest width E can be written as:

$$E = \frac{1}{8}\rho g H^2 \tag{27}$$

Insert Eq. 26 in Eq. 27 yields:

$$P = \frac{1}{8}\rho g H^2 C_g \cos\alpha \tag{28}$$

Assume no energy loss is caused by the bottom friction before the wave starts to break. Apply the energy conservation equation from the offshore wave to breaking wave yields:

$$H_o^2 C_{g,o} \cos\alpha_o = H_b^2 C_{g,b} \cos\alpha_b \tag{29}$$

Wave refraction needs to be considered when the waves approach the shoreline at an oblique angle. As the coastline outside the inlet is curved, it is divided into two areas. One is north of the inlet and one is south of the inlet (Figure 24). The bottom contours in each area are assumed to be parallel and straight to each shoreline for the simplification of the calculation, whereas bottom contours are usually curved in reality. When the bottom contours are not too complicated, this simplification can still produce a good estimation.

Figure 24. Representative shoreline orientation outside the inlet. Red lines are normal to the shorelines.

For each area, wave refraction is solved by Snell's law:

$$\sin\alpha_b = \frac{C_b}{C_o}\sin\alpha_o \tag{30}$$

where

α_b = the angle a breaking wave crest makes with the shoreline

α_o = the angle an offshore waves crest makes with the shoreline

C_b = the wave velocity at the breaking depth

C_o = the velocity of the offshore wave

For the convenience of calculation, the incoming wave direction is transferred using a local right-hand coordinate system. For each area, when wave crest is approaching perpendicularly to the shoreline, it is a 0-degree wave. From 0 degree to the right, waves have a positive angle. The wave angle is therefore calculated according to the new coordinate system:

$$\alpha_o = \theta_N - \theta_o \tag{31}$$

where

θ_N = the azimuth angle of the outward normal to the shoreline

θ_o = the azimuth angle with which the waves are approaching.

The group velocity is can be calculated by:

$$C_{g,i} = nC_i \tag{32}$$

where *i* stands for 0 or b, which is the offshore wave or the breaking wave, respectively.

And

$$n = \frac{1}{2}\left(1 + \frac{4\pi\frac{h_i}{L_i}}{\sinh\left(\frac{4\pi h_i}{L_i}\right)}\right) \tag{33}$$

In deep water, the wavelength L_0 (in meters) is calculated from wave period T (in seconds) by the follow equation:

$$L_o = \frac{gT^2}{2\pi} \tag{34}$$

Deep water wave celerity C_0 and deep water group velocity $C_{g,0}$ are given by:

$$C_o = \frac{L_o}{T} \tag{35}$$

$$C_{g,o} = \frac{1}{2} C_o \tag{36}$$

Use the three equations above yields $C_o = \sqrt{\frac{g L_o}{2\pi}}$ and $C_{g,o} = \frac{1}{2}\sqrt{\frac{g L_o}{2\pi}}$.

At breaking height, C_b and $C_{g,b}$ are assumed to be the same as in shallow water condition, thus $C_{g,b} = C_b = \sqrt{g h_b}$.

Insert the expression of $C_0, C_{g,0}, C_b$ and $C_{g,b}$ together with Eq. 29 to Eq. 28, the equation needs to be solved can be written as:

$$\left(\frac{h_b}{L_o}\right)^{5/2} \cos\left(\arcsin\left(\sqrt{2\pi}\sin\alpha_o\sqrt{\frac{h_b}{L_o}}\right)\right) = \left(\frac{H_o}{L_o}\right)^2 \frac{\cos\alpha_o}{\gamma_b^2 2\sqrt{2\pi}} \tag{37}$$

When breaking wave approaches at a small angle, i.e. $\cos\theta_b \cong 1.0$, the left side of Eq. 36 can by simplified as:

$$\frac{h_b}{L_o} = \left(\left(\frac{H_o}{L_o}\right)\frac{\cos\alpha_o}{\gamma_b^2 2\sqrt{2\pi}}\right)^{2/5} \tag{38}$$

Once the water depth at breaking h_b is obtained, the breaking wave height H_b can be calculated using Eq. 24.

Insert the expression of C_0 and C_b into Eq. 29, the angle a breaking wave crest makes with the shoreline is given by:

$$\alpha_b = \arcsin\left(\sqrt{2\pi}\sin\alpha_o\sqrt{\frac{h_b}{L_o}}\right) \tag{39}$$

Eq. 29, 34-38 are solved by the Fortran code with computed wave climate and α_o as input.

Longshore sediment transport

Hanson and Larson (1993) applied a model to calculate the net longshore sediment transport rate in the Falsterbo Peninsula. Their result is shown in Figure 25. According to Blomgren and Hanson (2000), this peninsula has not yet reached a final "equilibrium state" of its coastline.

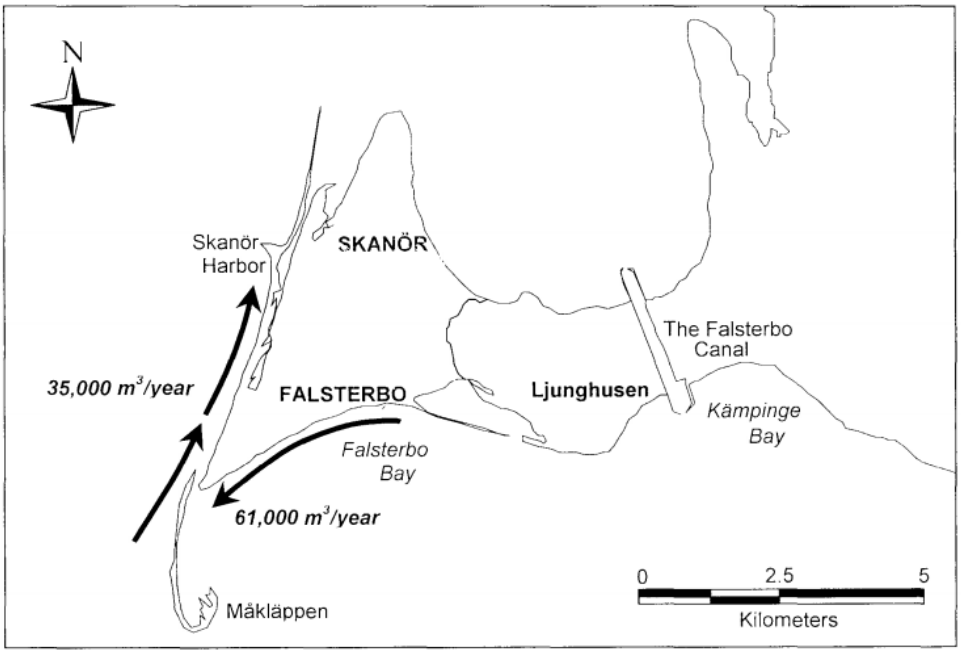

Figure 25. Net longshore sediment transport calculated by Hanson and Larson (1993).

In this report, the longshore sediment transport is calculated by the following method.

When wave approaches the shoreline with an oblique angle and breaks, sediments can be transported alongshore. This wave can be seen as the combination of two waves, one perpendicular to the shore and one alongshore.

The longshore wave energy flux (P_l) of the alongshore wave is calculated by the following equation (notation as before.):

$$P_l = \frac{\rho g}{16} H_b^2 C_{g,b} \sin(2\alpha_b) \tag{40}$$

The potential longshore sediment transport rate Q (in m^3/s) can be therefore calculated by:

$$Q = \frac{K}{g(\rho_s - \rho)(1-n)} P_l \tag{41}$$

where

K = longshore transport coefficient
ρ_s = density of the sediment grains, 2650 kg/m^3 for quartz-density sand
ρ = density of water, 1025 kg/m^3 for saltwater and 1000 kg/m^3 for fresh water
n = void space between particles, n=0.4

K is an empirical coefficient which differs for different locations. When using Hs (significant wave height) as H_b, K =0.39 is recommended. However, it is commonly believed that 0.39 is overestimated. When using $H_{b,rms}$ (root-mean-square wave height at breaking), K=0.92 is used instead (CEM, part 3, 2002). For the latter situation, Komar and Inman (1970) recommended to use K=0.77. This value is commonly used for longshore transportation calculation. After choosing the value of K, it needs to be calibrated according to local conditions. After calibration, K is usually between 0.2 to 1.0 (Hanson and Larson, 1992). In this report, significant wave height was used, and the K value was set to 0.15 as the same in the report from Hanson and Larson (1993).

For a sinusoidal wave, H_S and H_{m_0} can be considered to have the same value. When waves approach the shore, water depth becomes smaller and shoaling happens. This will twist the wave shape and results in different values of H_S and H_{m_0}. When water depth $h \geq 0.0975 T_p^2$ (T_P is the average peak spectral wave period), H_S and H_{m_0} are within 10% difference.

After the computation of the potential longshore sediment transport rate Q for each timestep (1 to N), the net longshore transport rate can be obtained by:

$$Q_{l,NET} = \frac{\sum_{1}^{N} Q}{N} \tag{42}$$

Notice that Q is assumed to be positive to the north and negative to the south. The gross transport rate is then obtained by:

$$Q_{l,GROSS} = \frac{\sum_{1}^{N} |Q|}{N} \tag{43}$$

Eq. 39-42 are solved by the Fortran code with computed wave climate and breaking wave conditions as input data. The average yearly net and gross longshore sediment transport rate and average monthly net and gross transport rate are calculated for the north of inlet and the south of inlet. The results can be found in Appendix. The average yearly net longshore sediment transportation rate is shown in the figure below.

Figure 26. Net longshore sediment transport rate (in m^3/year) along the west coast of Falsterbo.

The computed value shows that the net longshore sediment transportation direction is from south to the north along the shoreline, which is the same as the result from Hanson and Larson (1993). But the value is larger than their result. There might be because that when measuring fetch, they measured at different angles and got different fetch length as in this report. Larger volume of sediment transport is expected during winter, which is consistent with the wave conditions.

The twist angle of the shoreline results in a larger sediment transport rate in the south of the inlet than in the north of the inlet. This will result in accumulation of sand around the inlet mouth. When water exchange rate between the lagoon and the sea is not high enough to remove the sand, a sandy spit will grow around the inlet and further affect the water exchange rate.

Water level in the lagoon

In the coast of the Falsterbo Peninsula, effects from tides on water variation are negligible. Similarly, it is not very likely to be affected by tsunamis or strong tidal current. Instead, it is the large-scale water movement in the Baltic Sea and wind generated waves that dominate water level variation in this area.

Long-period resonant oscillations in large enclosed or partially enclosed water bodies are called seiches (SPM, 1984). Seiches in bays are usually generated by wind, air pressure changes or oscillation in the open sea transmitted through the inlet.

Saltwater/freshwater influx and outflux can also influence the water level in a lagoon. As mentioned before, the chloride concentration in the Flommen Lagoon (especially the southernmost part) is different from sea water. This indicates that groundwater infiltration has different influence on different part of the lagoon. Besides, surface runoff and evaporation can affect the water level.

Since the lagoon is rather long and has a complex shape, it was divided into five individual basins connected by channels with different frictional properties. The division can be seen in Figure 27. Water level is suspected to be different in different boxes. When water levels in all box are above a certain level, they can be merged. Similarly, when water level drops below this level, the merged box can split into small boxes again. The details will be introduced in the *Mathematical Model* chapter.

A digital elevation model (DEM) of the study area was provided by the Swedish company, SWECO. This DEM, using RH2000 reference system, shows topography data with the elevation above 0.1 m. From this DEM, surface area of elevation from 0.1 m to 1.5 m can be obtained, with a step of 0.1 m. Together with the field measurement data introduced in the next chapter, a lagoon surface area versus elevation plot is generated (Figure 28). It shows that the lagoon surface area changes quite a lot at different elevation. When water level is lower than 0.3 m, the lagoon surface area is less sensitive to water level variation in the lagoon. From 0.3 to 1.5 m, lagoon surface area will respond faster to water level variation.

Figure 27. Division of the lagoon.

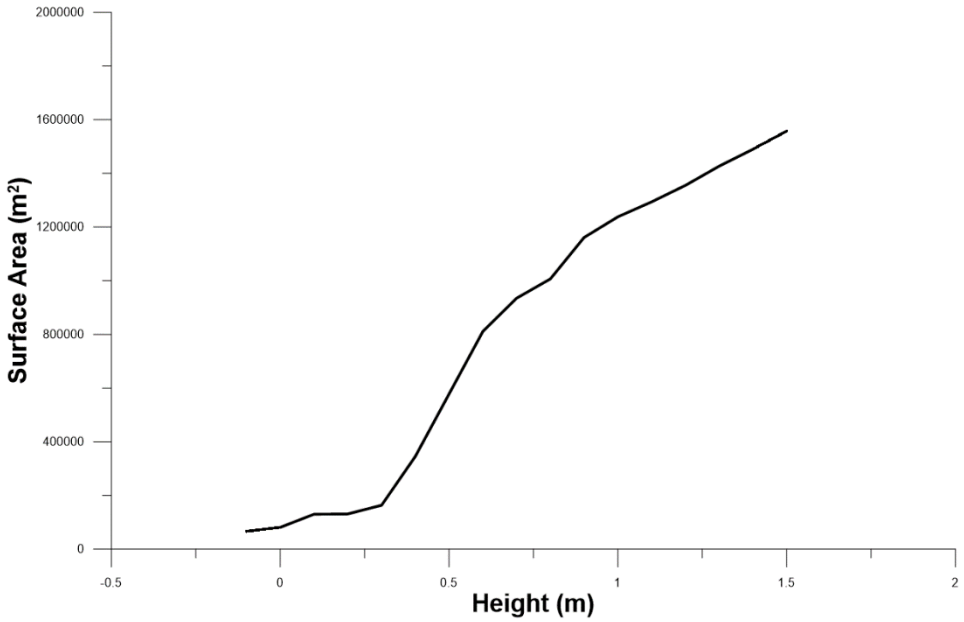

Figure 28. Lagoon surface area versus elevation.

Field measurements

Setup and procedure

Lagoon morphology measurement

The DEM only shows topography data with the elevation above 0.1 meter. In order to complete the data with elevation below 0.1 meters, one field campaign was performed on the 16th of April 2019.

The morphology survey was completed using a Topcon GR-3 GPS in Network-RTK mode using the SWEPOS real-time network, with a nominal uncertainty of measurement of ±1-2 cm (95%) in horizontal and 2-3 cm (95%) in vertical. The reference system used was RH2000. This device has a mobile data controller and a signal receiver (Figure 29). After clicking the "read" button on the controller, latitude, longitude and height can be recorded automatically. During this field campaign, the Topcon GR-3 receiver was attached to a 2-meter long stick. The height from the device to the tip of the stick was calibrated before the measurement. When measuring topography in the lagoon, the tip of the stick was always kept at the top of the solid sand bed. When the bottom of the lagoon was swampy and soft (deposition of sediments and organic matter), let the tip sink freely until it reached the solid sand bed, which is usually a decimetre from the top of the lagoon bottom.

Due to the time restriction, this measurement mainly focused on the northwest lagoon and the inlet (box 1 in Figure 27) because from the DEM the channels to other parts of the lagoon have rather high bottom elevation than 0.1 m. Measurement points can be found in Figure 31 (left).

Figure 29. Topcon FC-336 mobile data controller(left), Topcon GR-3 receiver (middle) and the 2-meter long stick (right).

Lagoon water lever variation measurement

With the aim of collecting water level variation in the lagoon, another measuring campaign was performed on the 6th of May 2019. The instrument used was a foldable wooden meterstick.

Figure 30. Foldable wooden meterstick.

Water level was measured at 5 different bridges (Figure 31, right) in the lagoon for five hours. The distance between the water surface in the lagoon and the bridge was measured on the bridge (the elevations of the bridges were measured during the first measuring campaign). A data series of water level variation was obtained.

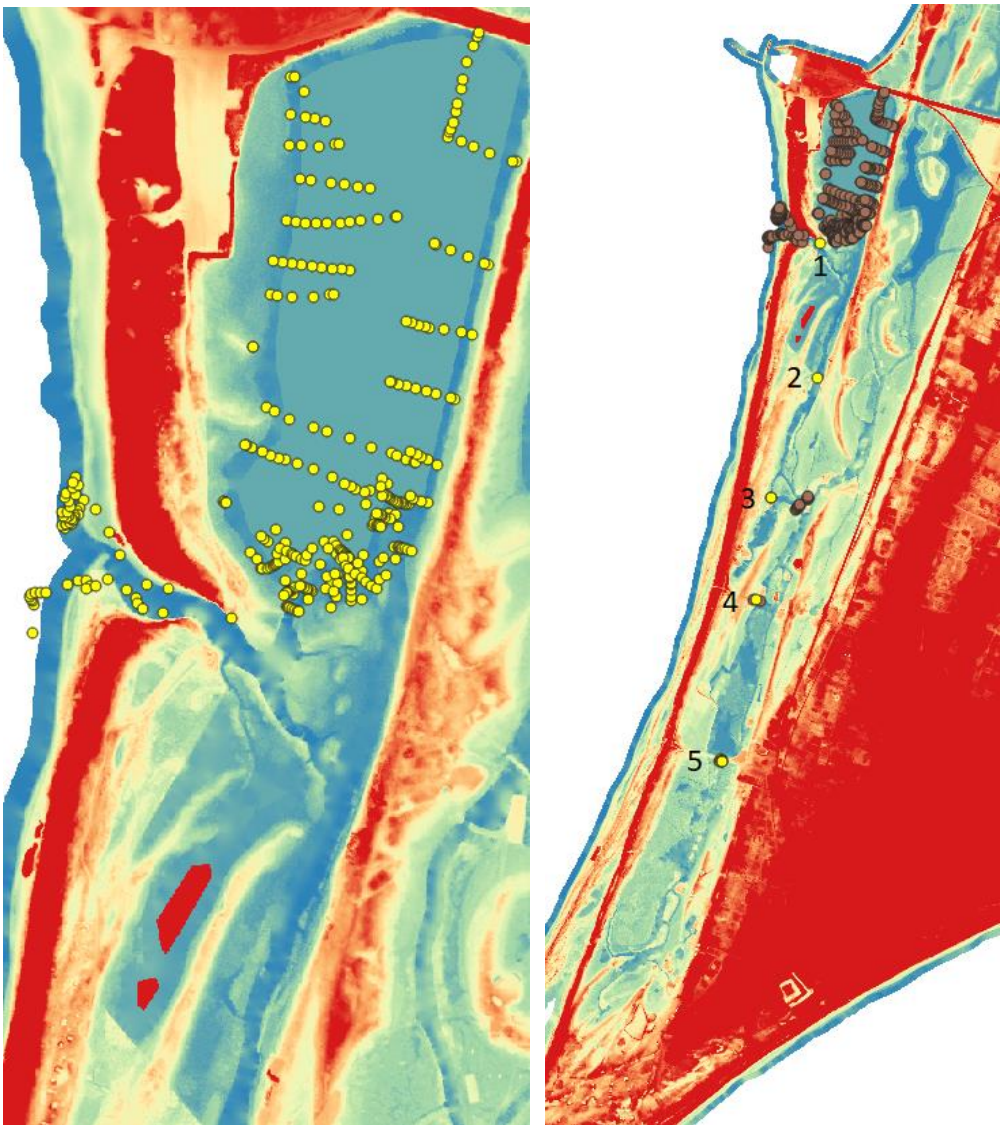

Figure 31. Map showing topography measurement sites (left) and water level variation measurement sites (right). Yellow dots stands for the measurement points.

Data collection and analysis

After the topography survey, the results were imported into QGIS and combined with the digital elevation model (DEM) to analyse the relationship

between the lagoon area and water level elevation in the lagoon. The surface area-elevation plot below was then generated and used in the mathematical model.

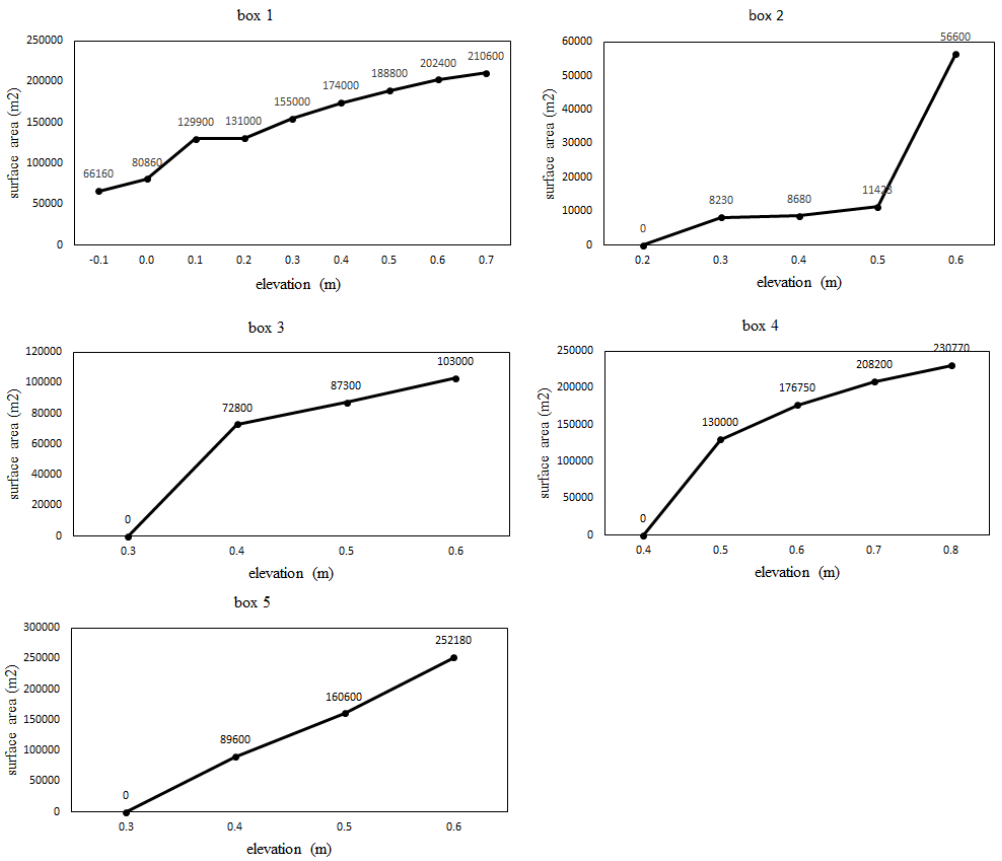

Figure 32. Surface area versus elevation of each box, data points start from the highest elevation of the channel to each box.

The water level variation measurement data was calculated according to RH2000 reference system. The sea level measurement data from SMHI is displayed using Coordinated Universal Time (UTC) and the measurements was recorded in Sweden time (UTC+2) so the time difference was also corrected. The sea level variation during the measurement period was approximately 1 decimetre, correspondingly the water level changes in the lagoon was not very significant. The measured water levels are shown as Table 2.

Table 2. Lagoon water level measurement. Reference system: RH2000.

Bridge number	Measuring time (UTC)	Water level (m)
1	2019-05-06 07:35	0,090
	2019-05-06 09:29	0,062
	2019-05-06 10:53	0,025
	2019-05-06 12:14	-0,015
2	2019-05-06 08:00	0,078
	2019-05-06 09:20	0,063
	2019-05-06 11:02	0,048
	2019-05-06 12:03	0,038
3	2019-05-06 08:15	0,072
	2019-05-06 11:10	0,054
4	2019-05-06 08:26	0,067
	2019-05-06 11:20	0,049
5	2019-05-06 08:40	0,033
	2019-05-06 11:33	0,038

Mathematical model

For the purpose of further understanding the water exchange process between the Flommen Lagoon and the sea, a mathematical model was developed and applied to simulate the response of the water level in the lagoon to the sea level. In this chapter, assumptions, governing equations for each box and development of the model and are introduced.

Assumptions

A mathematic model was developed using MATLAB to simulate the water exchange between the Flommen lagoon and the sea based on the classic work of Keulegan (1967). Water exchange between the lagoon and the sea was determined to be the only component of water exchange in this model. No river inflow, drainage discharge, evaporation or groundwater infiltration was considered in the model.

As mentioned before, the lagoon is very long and has a complex shape, so it was divided into five individual basins connected by channels with different frictional properties. Assume quasi-steady flow and uniform response in each box. When water level in the lagoon is above a certain level, boxes can be connected to each other; similarly, when water level drops to a certain level, jointed box can split into individual boxes. The detailed criteria can be found in Table 3.

Table 3. Box combination and separation criteria

Case	Water level	Description
1	in each box < 0.6 m	Every box is separated
2	0.6 m< in box 2, 3 and 5 <0.7 m	Box 1 and box 4 are separated, box 2, 3 and 5 become one box (namely box 235)
3	0.7 m< in box 1, 2, 3 and 5 < 0.8 m	Box 4 is separated, box 1, 2, 3 and 5 become one box (namely box 1235)
4	in each box > 0.8 m	All boxes become one box (namely box 12345)

At present, the sluice gate is closed when sea level is above 0.5 m to avoid flooding in the golf course. The lowest level of the gate is -0.35 m. Thus, there is no water inflow from the sea when sea level is below -0.35 m and no water exchange between the sea and the lagoon when sea level is above 0.5 m. Assume negligible frictional effect is caused by the sluice gate. When modelling with the scenario where the gate does not exist, the lowest level of the inlet channel was kept at -0.35 m, i.e., when sea level is below -0.35 m, there is no inflow from the sea.

The shape of the channel cross-section is usually irregular. To simplify the modelling process, the channel cross-section is assumed to be rectangular.

Governing equations

As in the Keulegan (1967) model, there are two governing equations used for each box: a water volume conservation equation and an energy conservation equation. In different cases, the inflow and outflow of the same box may be different, so different interpretation of equations are used.

Case 1

When water level in each box is below 0.6 m, no merge of the boxes will happen. The sketch of the model is shown in Figure 33.

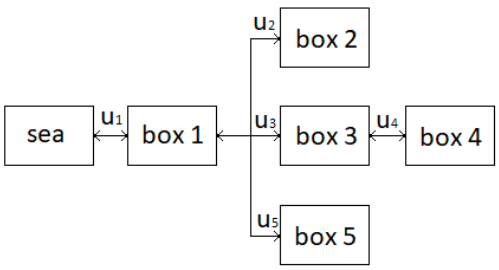

Figure 33. Sketch showing flow directions in case 1.

For box 1:

$$\frac{d(A_{L1}h_{L1})}{dt} = Q_{I1} - Q_{I2} - Q_{I3} - Q_{I15} \tag{44}$$

$$h_S = h_{L1} + k_{f_1} \frac{u_{I1}\left|u_{I1}\right|}{2g} \tag{45}$$

For box 2:

$$\frac{d(A_{L2}h_{L2})}{dt} = Q_{I2} \tag{46}$$

$$h_{L1} = h_{L2} + k_{f_2} \frac{u_{I2}\left|u_{I2}\right|}{2g} \tag{47}$$

For box 3:

$$\frac{d(A_{L3}h_{L3})}{dt} = Q_{I3} - Q_{I4} \tag{48}$$

$$h_{L1} = h_{L3} + k_{f_3} \frac{u_{I3}\left|u_{I3}\right|}{2g} \tag{49}$$

For box 4:

$$\frac{d(A_{L4}h_{L4})}{dt} = Q_{I4} \tag{50}$$

$$h_{L3} = h_{L4} + k_{f_4} \frac{u_{I4}\left|u_{I4}\right|}{2g} \tag{51}$$

For box 5:

$$\frac{d(A_{L5}h_{L5})}{dt} = Q_{I5} \tag{52}$$

$$h_{L1} = h_{L5} + k_{f_5} \frac{u_{I5}\left|u_{I5}\right|}{2g} \tag{53}$$

Case 2

When water level in box 2, 3 and 5 is between 0.6 to 0.7 m, box 2, 3 and 5 will become one box (namely box 235 in the model) while box 1 and box 4 remain separated.

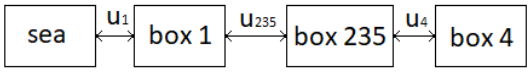

Figure 34. Sketch showing flow direction in case 2.

For box 1, the energy conservation equation has the same format as Eq. 45. The water volume conservation equation will be:

$$\frac{d(A_{L1}h_{L1})}{dt} = Q_{I1} - Q_{I235} \tag{54}$$

For box 235,

$$\frac{d(A_{L235}h_{L235})}{dt} = Q_{I235} - Q_{I4} \tag{55}$$

$$h_{L1} = h_{L235} + k_{f_{235}} \frac{u_{I235}|u_{I235}|}{2g} \tag{56}$$

Governing equations for box 4 are the same as in case 1.

Case 3

When water level in box 1, 2, 3 and 5 is between 0.7 to 0.8 m, box 1, 2, 3 and 5 become one box (namely box 1235 in the model) and box 1 remains separated.

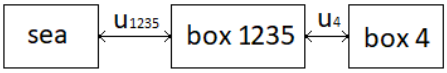

Figure 35. Sketch showing flow direction in case 3.

In this case, governing equations for box 1235 will be:

$$\frac{d(A_{L1235}h_{L1235})}{dt} = Q_{I1235} - Q_{I4} \tag{57}$$

$$h_S = h_{L1235} + k_{f_{1235}} \frac{u_{I1235}|u_{I1235}|}{2g} \tag{58}$$

Governing equations for box 4 are the same as in case 1.

Case 4

When water level in the whole lagoon is above 0.8 m, the lagoon is assumed to be one box, namely box 12345 in the model.

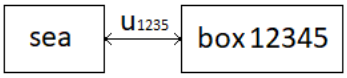

Figure 36. Sketch showing flow direction in case 4.

Governing equations for this case are:

$$\frac{d(A_{L12345}h_{L12345})}{dt} = Q_{I12345} \tag{59}$$

$$h_S = h_{L12345} + k_{f_{12345}} \frac{u_{I12345}|u_{I12345}|}{2g} \tag{60}$$

Numerical solutions

The governing equations can be solved using a numerical approach. The calculation steps of box 1 under case 1 is shown here as an example. Final equations to solve water level in each box can also be find in this section.

In the DEM, the minimum elevation of each box that had been measured is denoted as h_{cr}.

Explicit method

The flow velocity in inlet 1 can be solved from Eq. 45:

$$u_{I1} = \sqrt{\frac{2g}{k_{f_1}}} \frac{h_S - h_{L1}}{\sqrt{|h_S - h_{L1}|}} \tag{61}$$

Similarly, velocity of each inlet (u_I) can be calculated. Inflow to each box is thus calculated by the following equation:

$$Q_I = u_I A_I \tag{62}$$

Insert Q_I of each box and Eq. 61 to Eq. 44, the equation describing the water level variation in a box 1 can be written as (notation as before):

$$\begin{aligned} dh_{L1} = \frac{dt}{A_{L1}} \Big(& \frac{\sqrt{2g}}{k_{f_1}} \cdot A_{I1} \cdot \frac{h_S - h_{L1}}{\sqrt{|h_S - h_{L1}|}} - \frac{\sqrt{2g}}{k_{f_2}} \cdot A_{I2} \cdot \frac{h_{L1} - h_{L2}}{\sqrt{|h_{L1} - h_{L2}|}} \\ & - \frac{\sqrt{2g}}{k_{f_3}} \cdot A_{I3} \cdot \frac{h_{L1} - h_{L3}}{\sqrt{|h_{L1} - h_{L3}|}} - \frac{\sqrt{2g}}{k_{f_5}} \cdot A_{I5} \cdot \frac{h_{L1} - h_{L5}}{\sqrt{|h_{L1} - h_{L5}|}} \Big) \end{aligned} \tag{63}$$

The numerical scheme employed to solve this equation is explicit and new water levels are calculated based on the conditions displaced Δt/2 in time (Δt is the calculation time step). Eq. 63 is discretized as:

$$\begin{aligned} {h_{L1}}^{k+1} = {h_{L1}}^{k} + \frac{\Delta t}{A_{L1}^{k}} \Big(& \frac{\sqrt{2g}}{k_{f_1}} \cdot A_{I1} \cdot \frac{{h_S}^{k} - {h_{L1}}^{k}}{\sqrt{|{h_S}^{k} - {h_{L1}}^{k}|}} - \frac{\sqrt{2g}}{k_{f_2}} \cdot A_{I2} \cdot \frac{{h_{L1}}^{k} - {h_{L2}}^{k}}{\sqrt{|{h_{L1}}^{k} - {h_{L2}}^{k}|}} \\ & - \frac{\sqrt{2g}}{k_{f_3}} \cdot A_{I3} \cdot \frac{{h_{L1}}^{k} - {h_{L3}}^{k}}{\sqrt{|{h_{L1}}^{k} - {h_{L3}}^{k}|}} - \frac{\sqrt{2g}}{k_{f_5}} \cdot A_{I5} \cdot \frac{{h_{L1}}^{k} - {h_{L5}}^{k}}{\sqrt{|{h_{L1}}^{k} - {h_{L5}}^{k}|}} \Big) \end{aligned} \tag{64}$$

k = an index denoting a particular timestep

Δt = the length of the timestep

A_L^k = lagoon surface area corresponding to h_L^k. This equation is valid when $h_L^k > h_{cr}$ (when $A_L^k > 0$).

Using the same procedure, water level in each box under case 1 can be solved by the following equations:

$$h_{L2}^{\,k+1} = h_{L2}^{\,k} + \frac{\Delta t \cdot A_{I2}}{A_{L2}^{k}} \cdot \frac{\sqrt{2g}}{k_{f_2}} \cdot \frac{h_{L1}^{\,k} - h_{L2}^{\,k}}{\sqrt{\left|h_{L1}^{\,k} - h_{L2}^{\,k}\right|}} \tag{65}$$

$$h_{L3}^{\,k+1} = h_{L3}^{\,k} + \frac{\Delta t}{A_{L3}^{k}} \left(\frac{\sqrt{2g}}{k_{f_3}} \cdot A_{I3} \cdot \frac{h_{L1}^{\,k} - h_{L3}^{\,k}}{\sqrt{\left|h_{L1}^{\,k} - h_{L3}^{\,k}\right|}} - \frac{\sqrt{2g}}{k_{f_4}} \cdot A_{I4} \cdot \frac{h_{L1}^{\,k} - h_{L4}^{\,k}}{\sqrt{\left|h_{L1}^{\,k} - h_{L4}^{\,k}\right|}} \right) \tag{66}$$

$$h_{L4}^{\,k+1} = h_{L4}^{\,k} + \frac{\Delta t \cdot A_{I4}}{A_{L4}^{k}} \cdot \frac{\sqrt{2g}}{k_{f_4}} \cdot \frac{h_{L3}^{\,k} - h_{L4}^{\,k}}{\sqrt{\left|h_{L3}^{\,k} - h_{L4}^{\,k}\right|}} \tag{67}$$

$$h_{L5}^{\,k+1} = h_{L5}^{\,k} + \frac{\Delta t \cdot A_{I5}}{A_{L5}^{k}} \cdot \frac{\sqrt{2g}}{k_{f_5}} \cdot \frac{h_{L1}^{\,k} - h_{L5}^{\,k}}{\sqrt{\left|h_{L1}^{\,k} - h_{L5}^{\,k}\right|}} \tag{68}$$

For case 2, equations to be solved are:

$$h_{L1}^{k+1} = h_{L1}^{k} + \frac{\Delta t}{A_{L1}^{k}} \left(\frac{\sqrt{2g}}{k_{f_1}} \cdot A_{I1} \cdot \frac{h_{S}^{k} - h_{L1}^{k}}{\sqrt{\left|h_{S}^{k} - h_{L1}^{k}\right|}} - \frac{\sqrt{2g}}{k_{f_{235}}} \cdot A_{I235} \cdot \frac{h_{L1}^{k} - h_{L235}^{k}}{\sqrt{\left|h_{L1}^{k} - h_{L235}^{k}\right|}} \right) \tag{69}$$

$$h_{L235}^{k+1} = h_{L235}^{k} + \frac{\Delta t}{A_{L235}^{k}} \left(\frac{\sqrt{2g}}{k_{f_{235}}} \cdot A_{I235} \cdot \frac{h_{L1}^{k} - h_{L235}^{k}}{\sqrt{\left|h_{L1}^{k} - h_{L235}^{k}\right|}} - \frac{\sqrt{2g}}{k_{f_4}} \cdot A_{I4} \cdot \frac{h_{L235}^{k} - h_{L4}^{k}}{\sqrt{\left|h_{L235}^{k} - h_{L4}^{k}\right|}} \right) \tag{70}$$

$$h_{L4}^{\,k+1} = h_{L4}^{\,k} + \frac{\Delta t \cdot A_{I4}}{A_{L4}^{k}} \cdot \frac{\sqrt{2g}}{k_{f_4}} \cdot \frac{h_{L3}^{\,k} - h_{L4}^{\,k}}{\sqrt{\left|h_{L3}^{\,k} - h_{L4}^{\,k}\right|}} \tag{71}$$

For case 3, equations to be solved are:

$$h_{L1235}^{k+1} = h_{L1235}^{k} + \frac{\Delta t}{A_{L1235}^{k}} \left(\frac{\sqrt{2g}}{k_{f_{1235}}} A_{I1235} \frac{h_{S}^{k} - h_{L1235}^{k}}{\sqrt{\left|h_{S}^{k} - h_{L1235}^{k}\right|}} - \frac{\sqrt{2g}}{k_{f_4}} A_{I4} \frac{h_{L1235}^{k} - h_{L4}^{k}}{\sqrt{\left|h_{L1235}^{k} - h_{L4}^{k}\right|}} \right) \tag{72}$$

$$h_{L4}{}^{k+1} = h_{L4}{}^{k} + \frac{\Delta t \cdot A_{I4}}{A_{L4}^{k}} \cdot \frac{\sqrt{2g}}{k_{f_4}} \cdot \frac{h_{L3}{}^{k} - h_{L4}{}^{k}}{\sqrt{\left|h_{L3}{}^{k} - h_{L4}{}^{k}\right|}} \tag{73}$$

For case 4, equation to be solved is:

$$h_{L12345}^{k+1} = h_{L12345}^{k} + \frac{\Delta t \cdot A_{I12345}}{A_{L12345}^{k}} \cdot \frac{\sqrt{2g}}{k_{f_{12345}}} \cdot \frac{h_S^k - h_{L12345}^k}{\sqrt{\left|h_S^k - h_{L12345}^k\right|}} \tag{74}$$

Thus, water level in each box (h_L) can be calculated for each time step with water level in the sea (h_S) as an input.

Semi-explicit method

Using the above equations for the drying out situation should not cause any problems, but in case the lagoon starts to fill up again after being dry, *i.e.*, the surface area (A_L^k) starts to increase from 0, numerical problems may arise. Thus, a modified discretization of Eq. 63 is used to overcome this problem for *the first timestep* when an emptied lagoon is being filled up.

Instead of Eq. 64, a semi-explicit approach is used for the first timestep when the lagoon starts to fill up after being empty (after the first time step it should be possible to use Eq. 64 again). Eq. 63 is discretized in the following manner:

$$\begin{aligned} A_{L1}^{k+1} h_{L1}^{k+1} - A_{L1}^{k} h_{L1}^{k} = \frac{\Delta t}{A_{L1}^{k}} \Bigg(& \frac{\sqrt{2g}}{k_{f_1}} \cdot A_{I1} \cdot \frac{h_S{}^{k} - h_{L1}{}^{k}}{\sqrt{\left|h_S{}^{k} - h_{L1}{}^{k}\right|}} - \frac{\sqrt{2g}}{k_{f_2}} \cdot A_{I2} \cdot \frac{h_{L1}{}^{k} - h_{L2}{}^{k}}{\sqrt{\left|h_{L1}{}^{k} - h_{L2}{}^{k}\right|}} \\ & - \frac{\sqrt{2g}}{k_{f_3}} \cdot A_{I3} \cdot \frac{h_{L1}{}^{k} - h_{L3}{}^{k}}{\sqrt{\left|h_{L1}{}^{k} - h_{L3}{}^{k}\right|}} - \frac{\sqrt{2g}}{k_{f_5}} \cdot A_{I5} \cdot \frac{h_{L1}{}^{k} - h_{L5}{}^{k}}{\sqrt{\left|h_{L1}{}^{k} - h_{L5}{}^{k}\right|}} \Bigg) \end{aligned} \tag{75}$$

Developing Eq. 75 yields:

$$A_{L1}^{k+1}h_{L1}^{k+1} = A_{L1}^{k}h_{L1}^{k} + \frac{\Delta t}{A_{L1}^{k}}\left(\frac{\sqrt{2g}}{k_{f_1}}\cdot A_{I1}\cdot\frac{h_S{}^{k} - h_{L1}{}^{k}}{\sqrt{\left|h_S{}^{k} - h_{L1}{}^{k}\right|}} - \frac{\sqrt{2g}}{k_{f_2}}\cdot A_{I2}\cdot\frac{h_{L1}{}^{k} - h_{L2}{}^{k}}{\sqrt{\left|h_{L1}{}^{k} - h_{L2}{}^{k}\right|}}\right.$$
$$\left. - \frac{\sqrt{2g}}{k_{f_3}}\cdot A_{I3}\cdot\frac{h_{L1}{}^{k} - h_{L3}{}^{k}}{\sqrt{\left|h_{L1}{}^{k} - h_{L3}{}^{k}\right|}} - \frac{\sqrt{2g}}{k_{f_5}}\cdot A_{I5}\cdot\frac{h_{L1}{}^{k} - h_{L5}{}^{k}}{\sqrt{\left|h_{L1}{}^{k} - h_{L5}{}^{k}\right|}}\right) \quad (76)$$

Introducing a variable C^k to denote the term on the right-hand side and noting that $A_{L1}^{k} = 0$ when the empty lagoon starts filling up, the following equation is obtained:

$$A_{L1}^{k+1}h_{L1}^{k+1} = C_1^k \quad (77)$$

To solve this equation a relationship between A_L and h_L is needed. From the DEM we know that $A_L = 0$ for $h_L = h_{cr}$. If the next elevation at which we have a measured surface area is denoted h_m and the corresponding surface area $A_{L,m}$, then assuming a linear variation in A_L between h_{cr} and h_m gives:

$$A_{L1} = A_{L1,m}\frac{h_{L1} - h_{cr1}}{h_{m1} - h_{cr1}} \quad (78)$$

This equation is valid for $h_{cr} \le h_L \le h_m$. Using Eq. 78 in Eq. 77 yields:

$$A_{L1,m}\frac{h_{L1}^{k+1} - h_{cr1}}{h_{m1} - h_{cr1}}h_{L1}^{k+1} = C_1^k \quad (79)$$

Developing Eq. 79 produces a quadratic equation,

$$(h_{L1}^{k+1})^2 - h_{cr1}h_{L1}^{k+1} - \frac{C_1^k}{A_{L1,m}}(h_{m1} - h_{cr1}) = 0 \quad (80)$$

with the solution:

$$h_{L1}^{k+1} = \frac{1}{2} h_{cr1} + \sqrt{\left(\frac{1}{2} h_{cr1}\right)^2 + \frac{C_1^k}{A_{L1,m}} (h_{m1} - h_{cr1})} \tag{81}$$

Thus, during the first timestep when the empty box 1 is filling up, Eq. 81 is used to calculate the new water level in the lagoon. After that Eq. 64 is used again. Other boxes are simulated using the same solution.

Minimum area method

Due to the limitation of the DEM, the next surface area that can be examined after the minimum area is a quite large value. Therefore, during the first timestep after a box has dried, the surface area will experience a rapid increase from 0 which will introduce an instability in the model. When using the semi-explicit method, this will result in a noise in the output curve when the area of one box is zero.

To solve this problem, a minimum area of the lagoon was assumed with regards to the DEM as a third solution. When the elevation in a box drops below h_m, the surface area is assumed to be constant to the minimum area.

Thus, in the model, the minimum area method is used in combination with equations from the explicit method.

Water exchange and renewal time

For the simple case of a single lagoon with one inlet the expression for the renewal time (T_R) is shows as Eq. 2.

For the case of a tide generating this flow, the tidal prism (*i.e.*, the volume ΔV_T that flows in and out during a tidal cycle) divided by the tidal period (T_T) will yield the mean Q to be used to estimate T_R. For this case, the renewal time becomes:

$$T_R = \frac{V}{\Delta V / T_T} \tag{82}$$

If tide is not driving the water exchange, but more complex forcing conditions are controlling the exchange, which is the case for the Flommen

lagoon system, Q needs to be determined in a different way. Based on a long time period, the in- and outflow volume to the lagoon should to be the same; thus, the net volume change in the lagoon should be zero, which can be expressed through the flow according to:

$$\Delta V_{LT} = \int_0^{T_L} Q dt = 0 \tag{83}$$

where

ΔV_{LT} = the change in the net volume of the lagoon over a long time period T_L and
t = time.

If the in- and outflows are separated, then the above equation can be rewritten as:

$$\int_{Q>0} Q_P dt = \int_{Q<0} Q_N dt \tag{84}$$

where

Q_P = inflow, for which $Q > 0$
Q_N = outflow, with $Q < 0$.

The proper flow to represent the exchange flow (Q_m) in the renewal time T would be either the integral on the right- or left-hand side in the above equation divided by the time period considered (T_L). Another option to determine Q_m is to simply integrate the absolute value of the flow and divide by $2T_L$ according to:

$$Q_m = \frac{1}{2T_L} \int_0^{T_L} |Q| dt \tag{85}$$

For a discrete timeseries involving N values on Q, this expression can be written:

$$Q_m = \frac{1}{2N} \sum_1^N |Q| \tag{86}$$

For the study area, a complication when applying the concept of renewal time is to select a representative lagoon volume *V*, since the surface area varies markedly with the elevation. However, if different conditions regarding inflow cross section are investigated and it is assumed that the representative *V* does not differ between these conditions, it is sufficient to calculate Q_m for the different options and compare these values. For two conditions (denoted *1* and *2*), assuming that *V* does not vary too much between the two conditions, the definition of the renewal time yields:

$$\frac{T_{R1}}{T_{R2}} = \frac{Q_{m2}}{Q_{m1}} \tag{87}$$

Thus, if the exchange flow doubles, then the renewal time is halved.

In the model, Q is obtained by (denotes as before):

$$Q = u_I A_I \tag{88}$$

Parameters and input

This model used sea level observation data from SMHI as input data. In total, the observation records hourly sea level variation from February 1992 to the latest day. In the model, 10 days data (1st-10th January 2019) was chosen to representatively simulate the water exchange.

Model parameters were selected following estimates from Coastal Engineering Manual (2002).

The entrance energy loss coefficient k_{en} is recommended to be between 0.005 and 0.25 for flow entering an inlet channel, and less or equal to 0.05 for natural inlets, which are usually rounded at the entrance. In this model, k_{en} is chosen to be 0.05. The exit energy loss coefficient k_{ex} is taken to be 1 as the kinetic head is fully lost. Chow (1959) recommended a Manning's roughness coefficient n as 0.016 for open channel in hard-packed smooth sand. Considering that inlets usually has ripples or dune bottoms, it is recommended to use n=0.0225 by CEM (2002).

The timestep was chosen to be 10 seconds in order to get accurate and stable model output. Thus, the input data was interpolated accordingly.

Values of all the parameters can be find in Table 4.

Table 4. Parameters used in the model

Parameter	Value
k_{en}	0.05
k_{ex}	1
n	0.0225
timestep	10 seconds

Calibration and validation

Calibration and validation of the model were performed with measurement data on water level variation in the lagoon.

Due to the time limitation, only a short period of water level variation data was measured. This data series was used for the model calibration. Thus, no data was available for model validation. The validation was performed by comparing the model output generated by using calibrated values of parameters with the same measurement data.

The loss coefficient (k_f) of the lagoon inlet is the key parameter for calibration because the inlet morphology change is the dominate factor for the water exchange in this model. The was achieved by changing the value of *f*, k_{en} and *n*, then visually selecting the best fit between the simulation output and the measured data points. The calibration was mainly focused on box 1, 2, and 3 since potential groundwater infiltration is expected in box 4 and no measured data is corresponding to water level in box 5.

A series of numbers were examined during calibration. The figures below were chosen to show the changing pattern of simulation results versus *f* values. In these figures, k_{en}=0.05 *and* n=0.016 were used. *f* was calculated by Eq. 6.

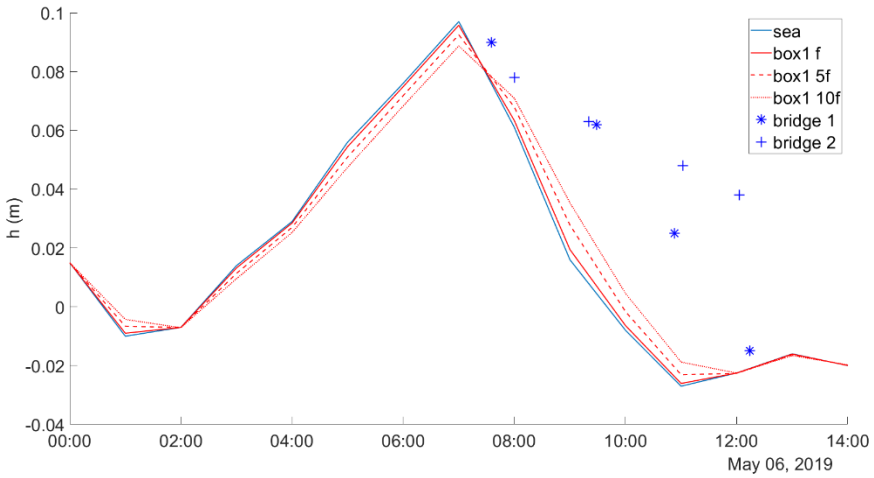

Figure 37. Calibration results- box 1

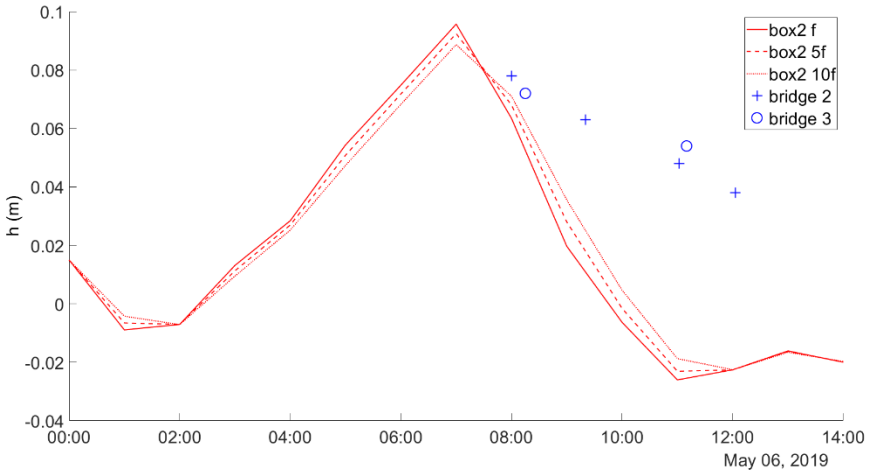

Figure 38. Calibration results- box 2

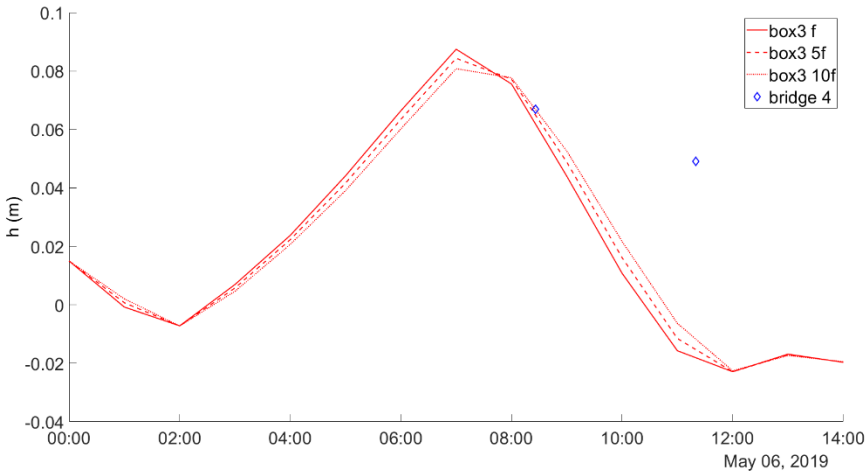

Figure 39. Calibration results- box 3

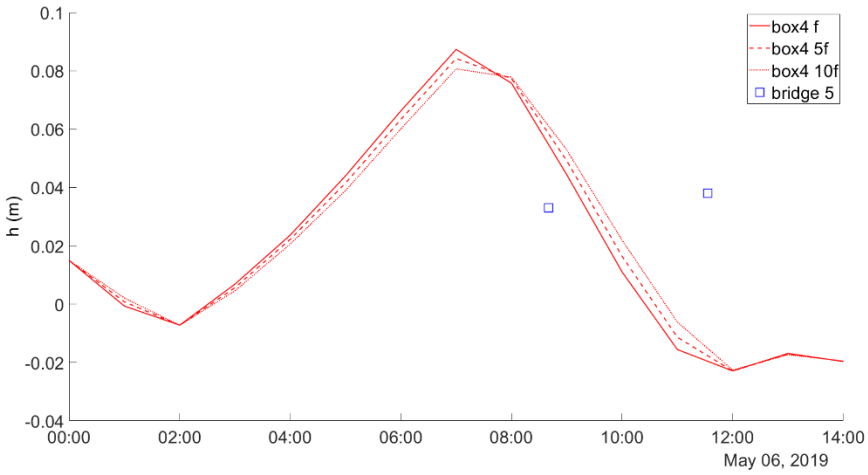

Figure 40. Calibration results- box 4

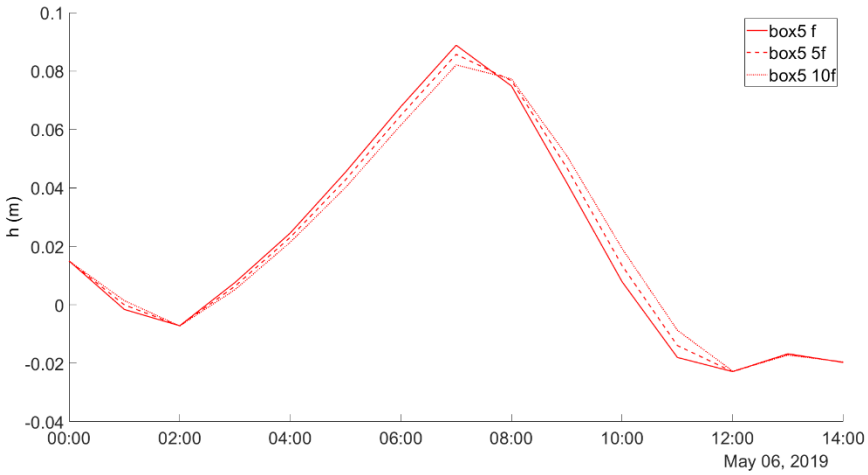

Figure 41. Calibration results- box 5 (no corresponding measured data)

According to the calibration plots, when k_{en}=0.05, n=0.016 and f=10f, the simulation results showed the best fits with the measured data point. It is worth noting that except for measurement on Bridge 4 (measuring location can be found in Figure 31), the water level variation data was measured not exactly in the lagoon. This is one reason why the simulation results cannot completely reproduce the measured data. Besides, measurement error is another reason.

After calibration, the model validation was performed with calibrated parameter values and the same measurement data. The simulation result is shown in Figure 42. The comparison of simulated water level with measured data in each box is shown in Figure 43. In general, after calibration, the model shows a good ability to simulate the water level variation in the lagoon even though at some data point time or phase lag between measured data and simulation values was observed.

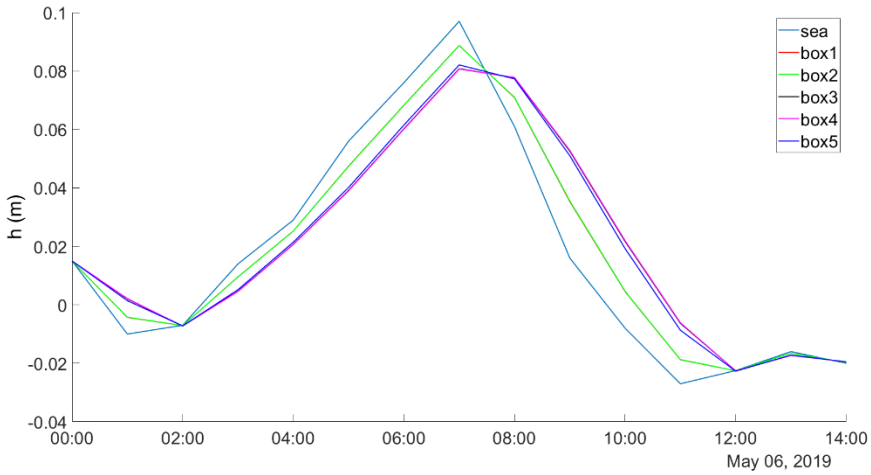

Figure 42. Validation: simulation results for the 6th May, generated by using calibrated parameters values.

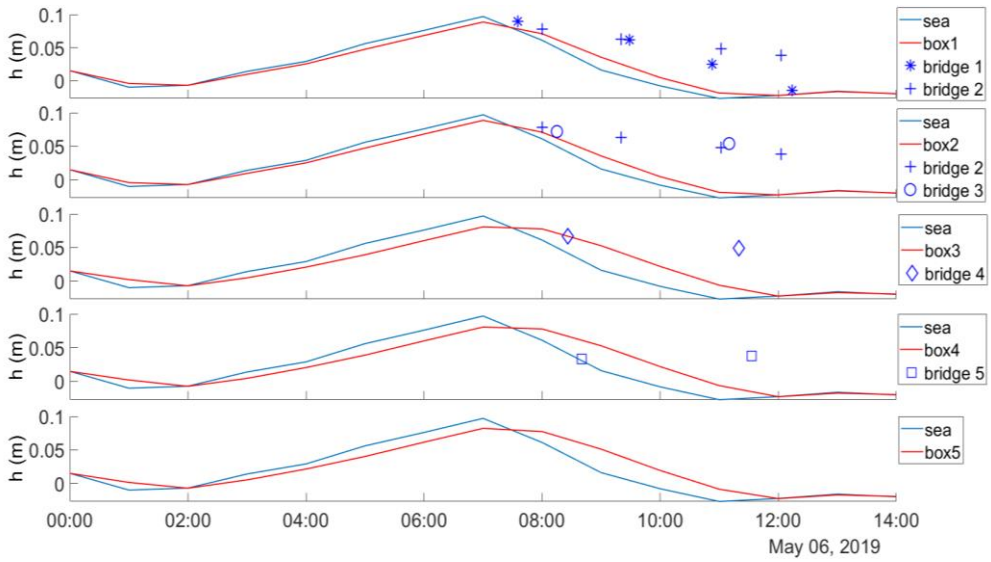

Figure 43. Validation: comparison of simulation results and measured data of each box

Simulation of different scenarios

Sinusoidal wave

After the model calibration and validation, a simple sinusoidal wave was used to test the responds between the lagoon water level and the sea water level.

Assume the incoming wave from the sea is a sinusoidal wave with an amplitude of 0.4 m and a period of 12 hours. The non-zero centre is set to 0.7 m. The wave is expressed as *hs=40*sin(w*x)+70*. The sea water level is thus oscillating between 0.3 to 1.1 meter.

As is shown in Figure 44, under the condition where the sluice gate is under operation, merge of box 2, 3 and 5 happens at the beginning. After a period of revolution from the gate closed, water level in every box tends to become identical and remains below 0.4 m. Very large phase lag and time lag between sea water level and lagoon water level are expected.

Under the condition where the gate is assumed to be removed, with the same incoming wave, smaller phase lag and time lag are expected. Boxes start to merge when water level in boxes reaches a certain level. Due to the sudden increase of surface area when boxes start to merge, the water level in the merged box will experience an instant increase. The highest water level in the lagoon is simulated to be 0.84 m, which is about 0.5 m higher than with the gate under operation.

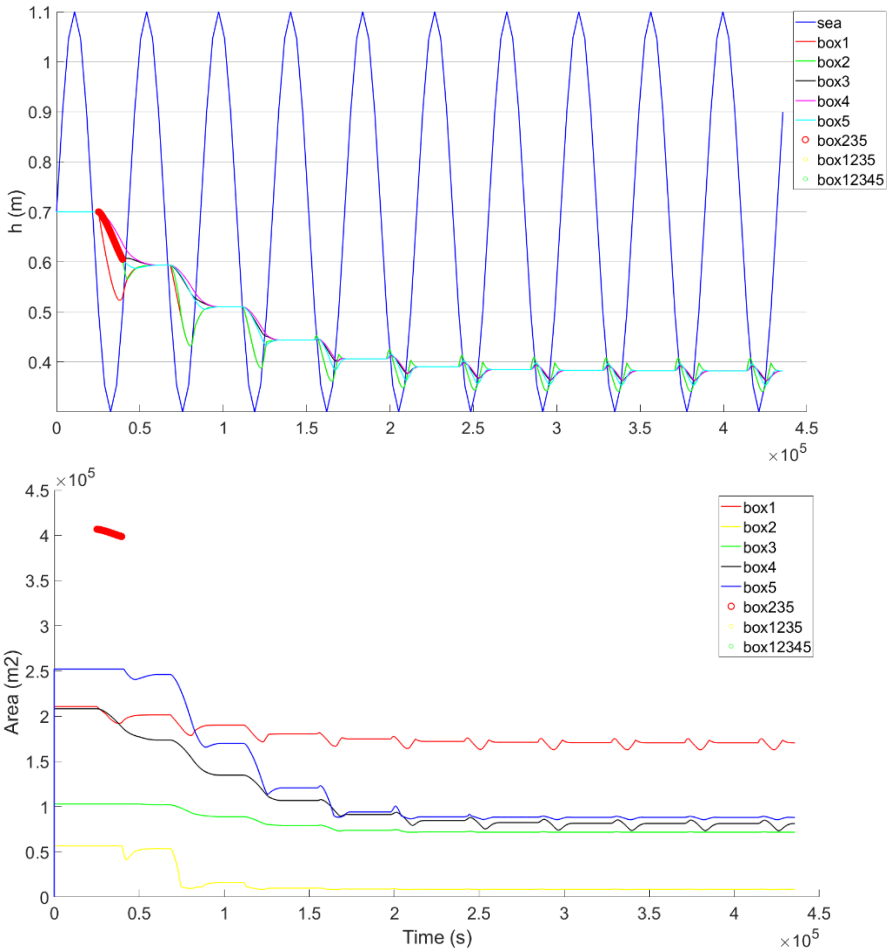

Figure 44. Simulation of lagoon water level and surface area from a sinusoidal wave, with the sluice gate under operation.

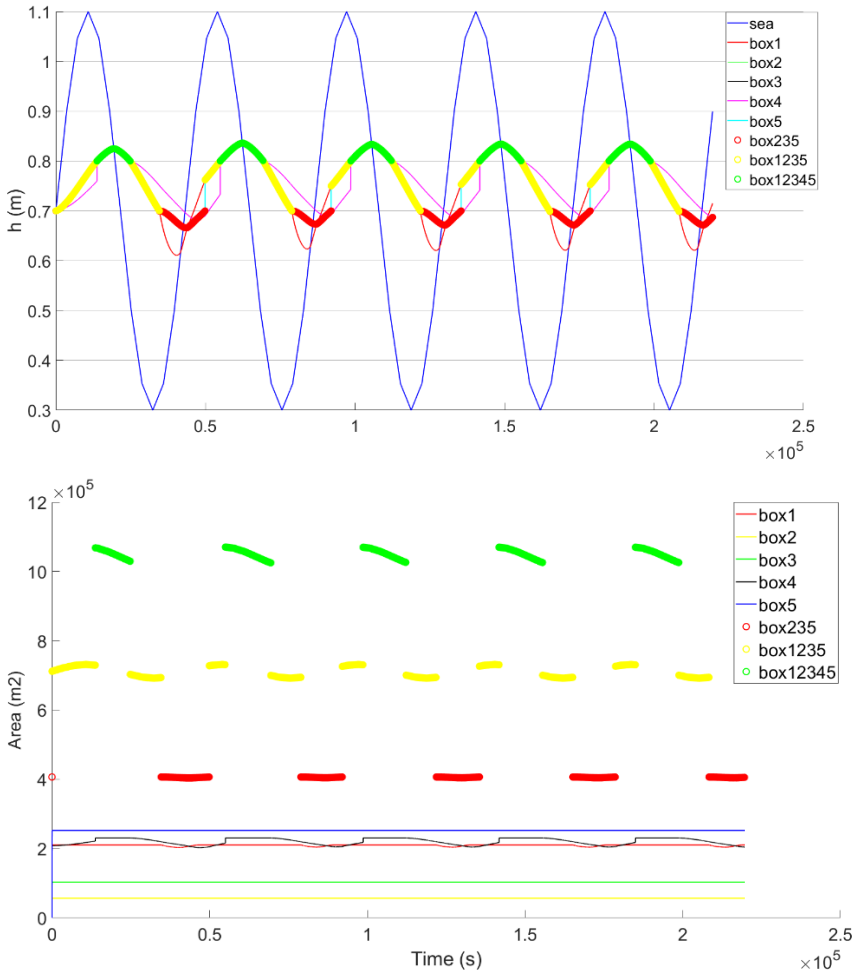

Figure 45. Simulation of lagoon water level and surface area from a sinusoidal wave, without the sluice gate.

Inlet geometry

The impact of the inlet (between the lagoon and the sea) morphology change and the spit growth around the inlet is studied by varying the inlet cross-section area in the model. Sea level observation data was used as input. The cross-section area was halved and doubled.

The cross-section area changing has no significant influence on the water level in the lagoon. But it affects the water exchange rate. Larger cross-

section area results in larger water exchange. Half the cross-section area decreases the gross exchange rate of 39.2% and double cross-section area increases the gross exchange rate of 15.3%.

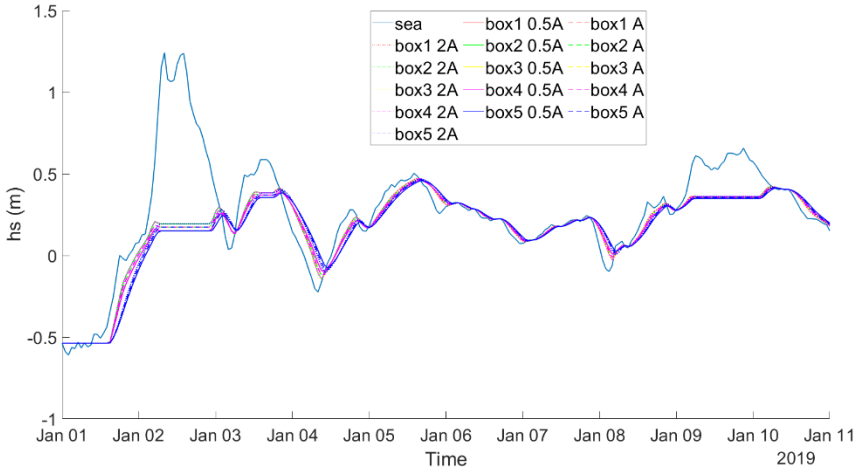

Figure 46. Simulation results of water level in the lagoon with data from 1st-10th January 2019. A- the lagoon inlet cross-section area based on inlet geometry from the DEM.

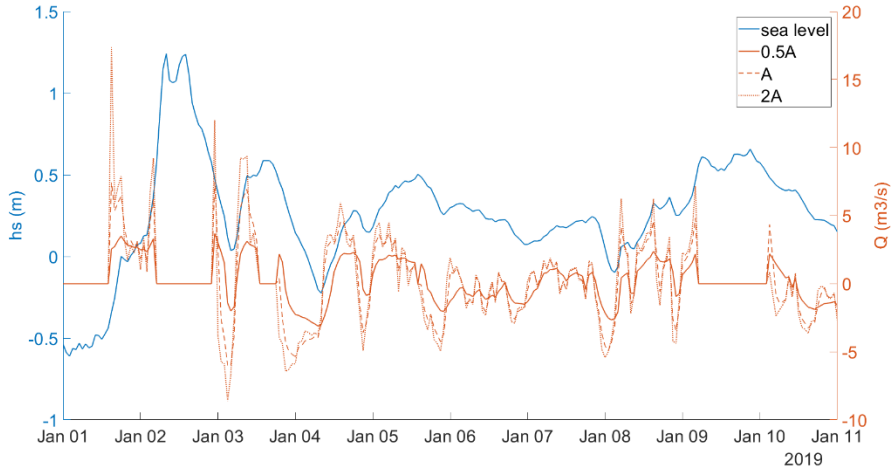

Figure 47. Simulation results of water exchange with data from 1st-10th January 2019. A- the lagoon inlet cross-section area based on inlet geometry from the DEM.

Table 5. Water exchange rate. Generated from 10 days data of 1st to 10th January, 2019. A- lagoon inlet cross-section area based on inlet geometry from the DEM.

Exchange rate Q (m^3/s)	0.5A	A	2A
Average positive	1.6533	2.5131	2.9754
Average negative	-1.3644	-2.4537	-2.7534
Average net	0.2137	0.1972	0.2132
Average gross	3.0177	4.9669	5.7288

Effect of the sluice gate

In this section, the effect of the sluice gate is discussed regarding to water exchange rate and extreme events. As mentioned before, the sluice gate on the lagoon inlet is closed when water level in the sea is above 0.5 m and the lowest level of the gate is -0.35 m.

Water exchange rate

Sea level observation data from SMHI of January 1st, 2019 to January 10th, 2019 was selected to representatively simulate the water exchange between the lagoon and the sea.

In general, without the sluice gate, larger inflow and outflow are expected. This will increase the amount of water exchanged between the lagoon and the sea. Without the sluice gate, gross water exchange rate is 31.6% larger than with the gate under operation. Average net exchange rate in the modelling results is not zero while based on a longer time period, no water accumulation is expected.

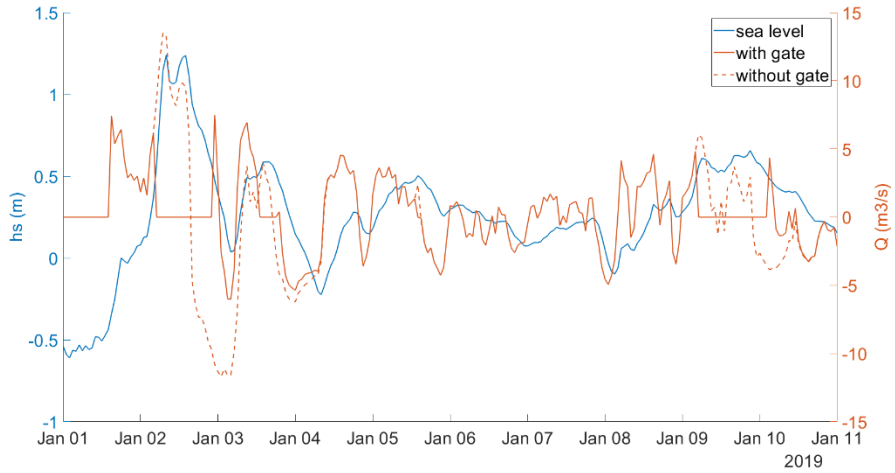

Figure 48. Water exchange rate with and without the sluice gate. Generated from 10 days data of 1st to 10th January, 2019. Q is possitive when water flows into the lagoon.

Table 6. Water exchange rate. Generated from 10 days data of 1st to 10th January, 2019.

Exchange rate Q (m^3/s)	With the sluice gate	Without the sluice gate
Average possitive	2.5131	3.0579
Average negative	-2.4537	-3.4784
Average net	0.1972	-0.0073
Average gross	4.9669	6.5363

Extreme events

There is very limit data record about extreme events in Falsterbo. Therefore, a sinusoidal wave with a large amplitude was used to simulate the effect of the gate when extreme event happens.

Fredriksson et. al (2016) used a general extreme value (GEV) model to predict the extreme water level in the Falsterbo Peninsula. Sea water level observation data in Skanör station is not long enough (1992-2019) to accurately predict a 100-year event. Therefore, the calculation was based on the sea level variation data from three observation stations around the Swedish southern coast: Skanör, Klagshamn and Ystad. According to them, an extreme event with a 100-year return period is calculated to exceed 1.8 m

(reference system: RH2000). This value is used in this section to simulate the effect of the sluice gate.

Figure 49. Location of Skanör, Klagshamn and Ystad sea level observation station (Fredriksson et. al, 2016).

The sinusoidal wave can be expressed as*: hs=80*sin(w*x)+110;* with a period of 12 hours. This will generate a wave with height above 1.8 m for about 2 hours continuously. With the gate being operated at t=0, water level in the lagoon will gradually increase but remain below 0.5 m. In this situation, no severe damaged will be caused in the golf courses and the adjacent area.

Without the sluice gate, the water level in the lagoon will oscillate between 0.9 to 1.2 m during this extreme event. The water level in the lagoon will exceed 1.1 m for about 4 hours. From the DEM, part of the coastline will be flooded, but the lagoon still shows a good ability to protect the adjacent inland area from flooding. However, the golf courses will be flooded in this situation.

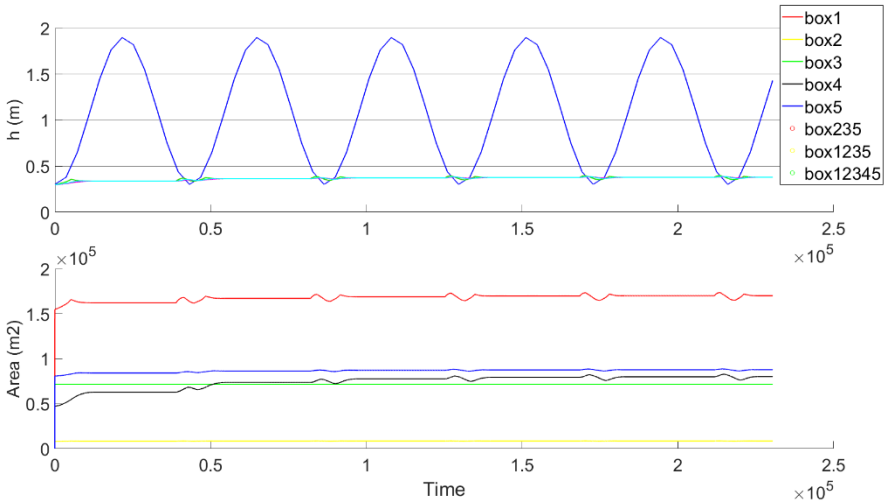

Figure 50. Lagoon water level changes during a 100-year return period event, with gate closed at t=0.

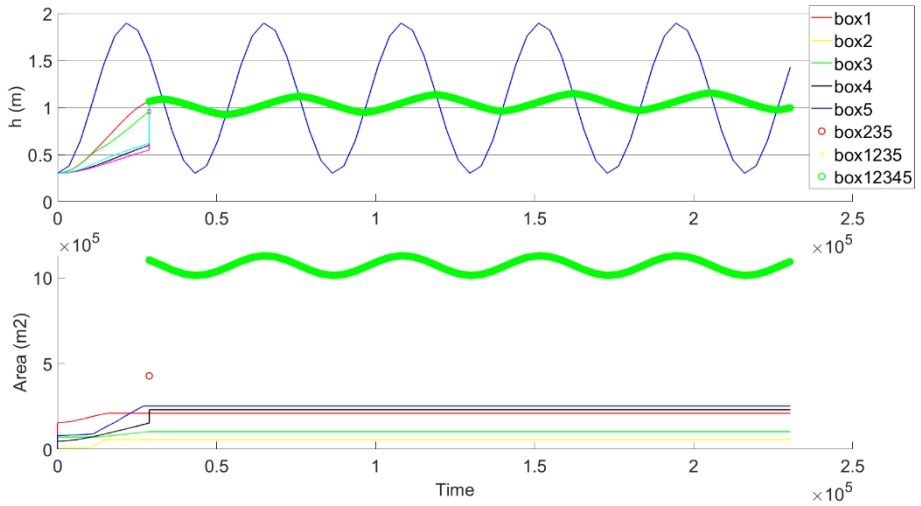

Figure 51. Simulation of water level changes during a 100-year event, without the sluice gate.

Figure 52. Area with elevation below 1.1 m (in black colour) (RH 2000).

A second inlet

During years there has always been a discussion about opening a second inlet to the Flommen Lagoon. One suggestion is to dig another inlet between box 1 and the ocean. In this section, the effect of having a second inlet was simulated both with a sinusoidal incoming wave and 10 days sea water level measurement data from Skanör station.

The second inlet was assumed to have the same properties as the original inlet, and they both have sluice gates. This will add another Q_I for box 1 in Eq. 1. In the model, this has the same effect as double the inlet cross-section area of inlet 1. The sinusoidal wave used here is the same as in the *Sinusoidal wave* section. This wave has a formula of *hs=40*sin(w*x)+70.*

According to the simulation output, with the incoming sinusoidal wave, the water level in the lagoon will eventually remain between 0.4 to 0.45 m with

two inlets (see Figure 53). This value is slightly higher than with one inlet, where the water level in the lagoon is expected to remain below 0.4 m (see Figure 44). A smaller time lag is also observed with two inlets.

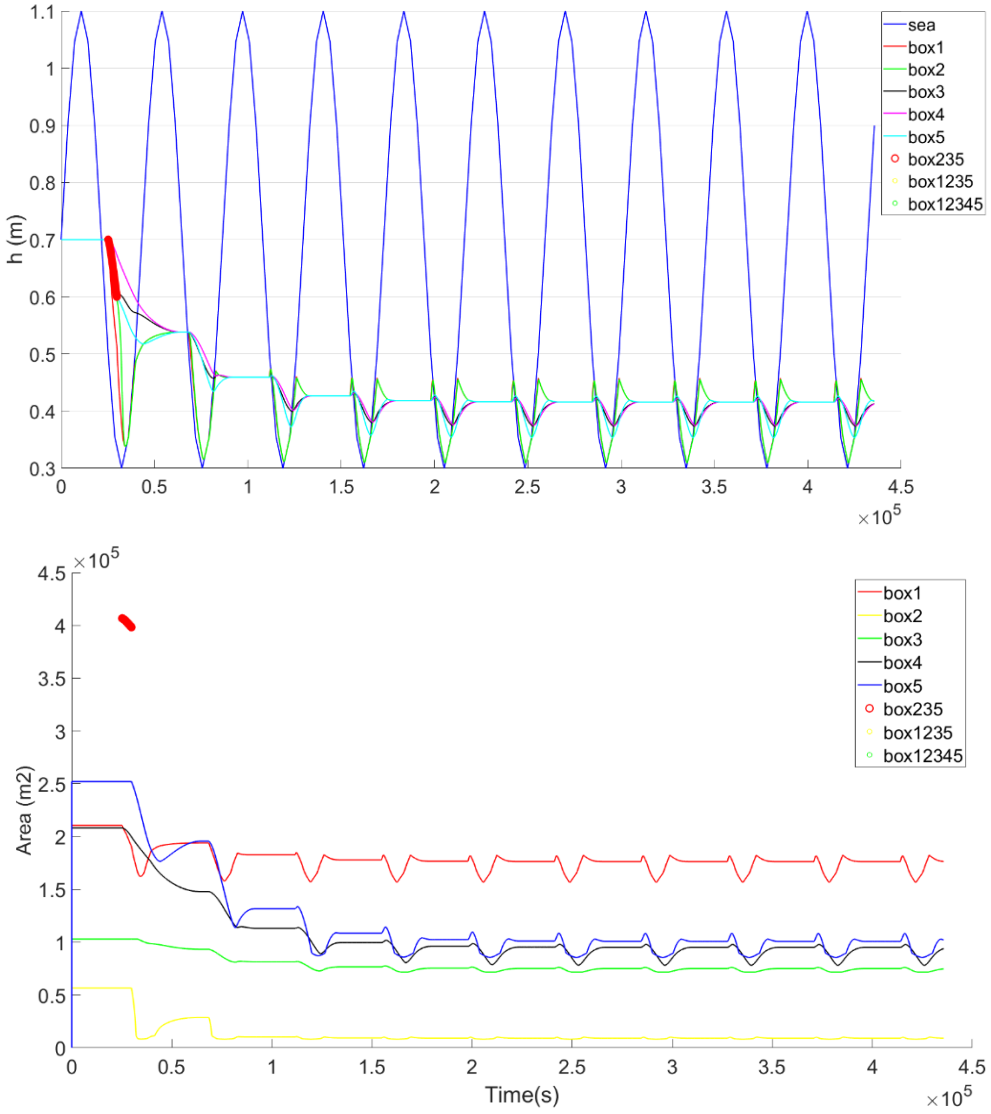

Figure 53. Simulation results of two inlets, with a sinusoidal incoming wave.

The same trend was also observed when simulating with observation data Skanör sea level measurement station. Data from January 1st, 2019 to January

10^{th}, 2019 was selected. A second inlet will result in a faster respond to sea level variation and a higher water level in the lagoon when the gate is closed.

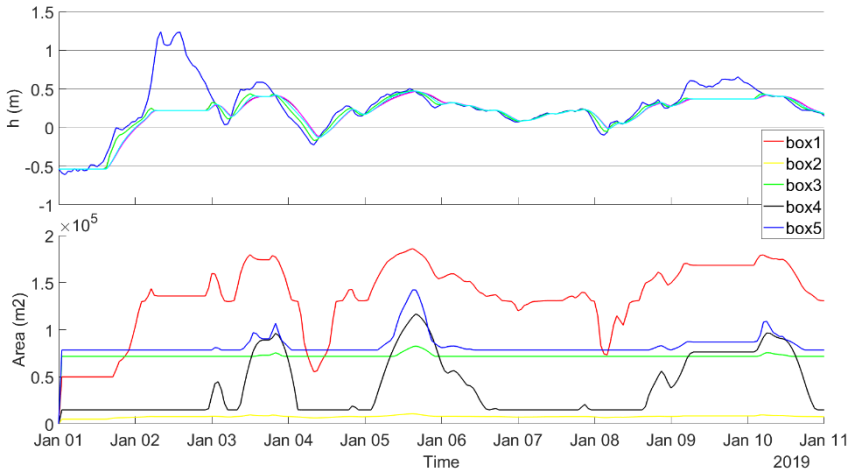

Figure 54. Simulation results of one inlet, with 10-day sea level variation data.

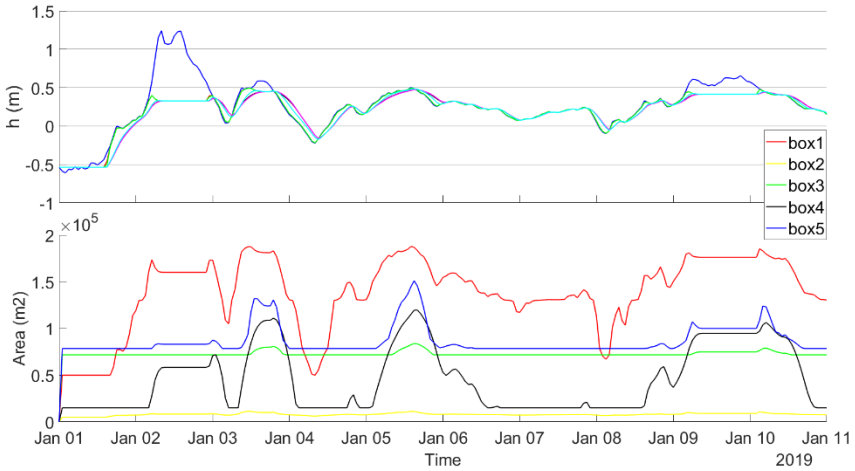

Figure 55. Simulation results of two inlets, with 10-day sea level variation data.

When the gate is closed, the volume of water outflow and inflow are significantly higher with two inlets than with one inlet. When the gate is open, water exchange rates are rather similar with one or two inlets. For this data

period, average gross water exchange rate with 2 inlets is 15.3% higher than with one inlet.

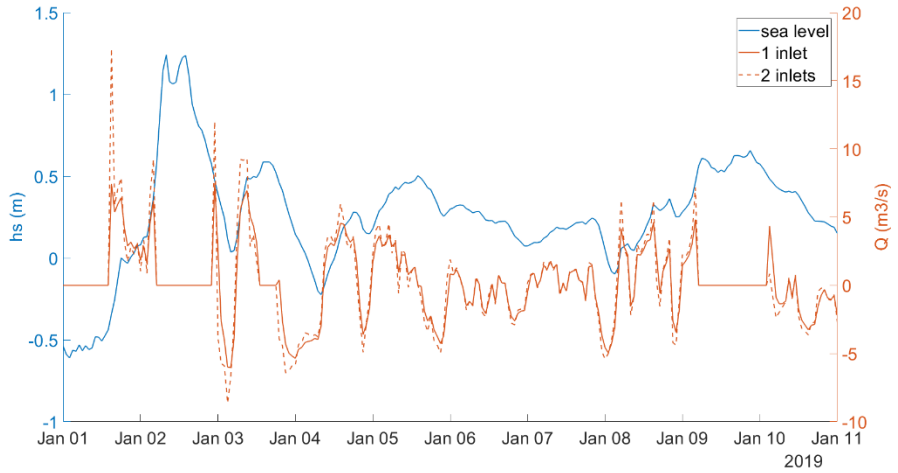

Figure 56. Water exchange rate with one inlet and two inlets.

Table 7. Water exchange rate. Generated from 10 days data of 1st to 10th January, 2019.

Exchange rate Q (m^3/s)	1 inlet	2 inlets
Average possitive	2.5131	2.9754
Average negative	-2.4537	-2.7534
Average net	0.1972	0.2132
Average gross	4.9669	5.7288

Conclusions

The aim of this report was to study the physical processes governing the water exchange at the Flommen lagoon. These physical processes studied here include the regular dredging of the inlet channel, longshore sediment transport and the operation of the sluice gate. This was achieved by qualitatively analysing the influence of sediment transport on inlet geometry, numerically modelling with different scenarios and quantitively analysing the effects of the inlet geometry and the sluice gate on lagoon water level variation and water exchange rate. Furthermore, the possible influence of constructing a second opening between the sea and the lagoon was also studied.

The longshore sediment transport rate is 61 000 m^3/year in the south of the inlet and 13 000 m^3/year in the north. This will increase the tendency of sand accumulation around the inlet and the reduce the inlet area. Inlet geometry has no significant influence on the water level in the lagoon, but it will significantly influence the water exchange rate. Based on the simulation result of ten days sea level variation data, halve the cross-section area decreases the gross water exchange rate by 39.2% and double cross-section area increases it by 15.3%.

The sluice gate on the current inlet generates smaller water exchange than without the gate. Without the sluice gate, gross water exchange rate is 31.6% larger than with the gate under operation. The sluice gate also deceases the threaten of flooding in adjacent areas when extreme event happens. Without the gate, the golf courses around the lagoon will be totally flooded if an event with a return period of 100-year happens.

A second inlet with the same characteristics as the current one has a similar influence to double the cross-section area. With two inlets, lagoon water level was modelled to be slightly higher than with one inlet. For the 10-day sea level variation data period, average gross water exchange rate with 2 inlets was modelled to be 15.3% higher than with one inlet.

Reflection

Due to its complex shape, the Flommen Lagoon was divided into five boxes to model the responds of lagoon water level to sea level. Water level in each box was assumed to be the same at every point. However, during the second field measurement, it was noticed that water level is slightly different at different location in one box. In the future the model can be improved by dividing the lagoon into finer mesh grids if the flow direction can be better defined.

Besides, there is no available data of the water level variation in the lagoon. Due to the time limitation, only data for a few hours was recorded during the field campaign. The model can be better calibrated and validated if more data is gathered in the future.

The influence of groundwater infiltration was neglected in the model whereas in the southern part of the lagoon it has some influences on the water salinity. This can be considered if more information about groundwater infiltration in this area is combined.

References

Blomgren, S. and Hanson, H., 2000. Coastal geomorphology at the Falsterbo Peninsula, Southern Sweden. *Journal of Coastal Research, 16*(1), 15-25.

Blomgren, S., Larson, M. And Hanson, H., 1999. Numerical modelling of the wave climate in the Southern Baltic Sea, *Journal of coastal research 17*(2), pp. 342–352.

Chow, V. T., 1959. *Open-channel hydraulics* (Vol. 1). New York: McGraw-Hill.

Dahlerus, C.J. and Egermayer, D., 2005. *Run-up and Sand Dune Erosion Along the Coast of Ystad–Present Situation and Future Scenarios*. Lund University.

Davidsson, J.Å.K., 1963. *Littoral processes and morphology on Scanian flat-coasts, particularly the peninsula of Falsterbo*. Royal University of Lund Department of Geography: CWK Gleerup.

Emanuelsson, D. and Mirchi, A., 2007. *Impact of coastal erosion and sedimentation along the northern Sinai coast*. Lund University.

Engineers, U.A.C.O., 2002. Coastal Engineering Manual. Engineer Manual 1110-2-1100. *US Army Corps of Engineers, Washington, DC*.

Fredriksson, C., Tajvidi, N., Hanson, H. and Larson, M., 2016. Statistical Analysis of extreme sea water levels at the Falsterbo peninsula, South Sweden. *VATTEN—Journal of Water Management and Research, 72*, pp.129-42.

Gärdenfors, U. ed., 2010. *Rödlistade arter i Sverige 2010: the 2010 red list of Swedish species*. Artdatabanken i samarbete med Naturvårdsverket. (In Swedish)

Gärdenfors, U., Simán, S. and Lundkvist, K., 2005. *Rödlistade arter i Sverige 2005*. ArtDatabanken i samarbete med Naturvårdsverket. (In Swedish)

Hanson, H., 2007. Falsterbo Peninsula (Sweden). [pdf]. Available at: <http://www.eurosion.org/shoreline/54falsterbo.html> [Accessed 20 April 2019].

Hanson, H. and Larson, M., 1993. *Sandtransport och Kustutveckling vid Skanör/Falsterbo*. Lund: Lund University. (In Swedish)

Keulegan, G. H. 1967. *Tidal Flow in Entrances Water-Level Fluctuations of Basins in Communications with Seas*. Technical Bulletin No. 14, Committee on Tidal Hydraulics, U.S. Army Engineer Waterways Experiment Station, Vicksburg, MS.

Kjerfve, B., 1986. Comparative oceanography of coastal lagoons. In *Estuarine variability* (pp. 63-81). Academic Press.

Kjerfve, B. and Magill, K.E., 1989. Geographic and hydrodynamic characteristics of shallow coastal lagoons. *Marine geology*, *88*(3-4), pp.187-199.

Manual, S.P., 1984. US Army Coastal Engineering Research Center. *Fort Belvoir*, *1*.

Nelson, H., 1923. Från skånska kuster och stränder. *Skånes Natur* 11: 3- 1 5. Lund. (In Swedish)

Nerheim, S., Schöld, S., Persson, G. and Sjöström, Å., 2017. *Framtida havsnivåer i Sverige*. (In Swedish)

O'Brien, M. P. 1931. "Estuary Tidal Prisms Related to Entrance Areas," *Civil Engineering*, pp 738-739.

Ohlsson, A., Asp, M., Berggreen-Clausen, S., Berglöv, G., Björck, E., Johnell, A., Mårtensson, J., Nylén, L., Persson, H. and Sjökvist, E., 2015. *Framtidsklimat i Skånas län-enligt RCP-scenarier*. SMHI. (In Swedish)

Takeoka, H., 1984. Fundamental concepts of exchange and transport time scales in a coastal sea. *Continental Shelf Research*, *3*(3), pp.311-326.

Zimmerman, J.T.F., 1976. Mixing and flushing of tidal embayments in the western Dutch Wadden Sea part I: Distribution of salinity and calculation of mixing time scales. *Netherlands Journal of Sea Research*, *10*(2), pp.149-191.

Appendix

Calculation for sediment transport rate

Table A-1. Yearly transport rate in m^3/year, south of the inlet.

Year	Positive Q	Negative Q	Net Q	Gross Q
1974	115642	-36490	79152	152132
1975	133244	-41620	91624	174864
1976	90949	-38457	52492	129405
1977	124189	-38222	85967	162411
1978	95948	-44674	51274	140622
1979	106483	-29721	76761	136204
1980	134950	-51934	83016	186884
1981	100918	-45095	55823	146013
1982	108319	-18983	89337	127302
1983	145311	-40880	104431	186192
1984	108712	-33908	74804	142620
1985	86752	-37974	48778	124725
1986	85239	-25763	59476	111002
1987	67079	-21734	45345	88813
1988	87115	-31942	55174	119057
1989	80168	-30971	49197	111139
1990	139010	-27879	111131	166889
1991	84237	-19613	64624	103850
1992	83142	-22985	60157	106127
1993	52151	-19714	32437	71865
1994	64304	-27560	36744	91864
1995	57199	-32951	24248	90150
1996	44974	-12262	32712	57235
1997	64102	-32596	31506	96699
1998	114259	-23758	90501	138017
1999	103069	-19856	83213	122925
2000	91796	-25184	66612	116980
2001	54523	-28535	25988	83058

2002	63982	-20305	43677	84287
2003	37609	-35302	2307	72912
2004	75436	-27123	48314	102559
2005	73379	-16697	56682	90077
2006	59550	-12098	47451	71648
2007	107639	-45630	62009	153269
2008	135071	-26307	108764	161378
2009	86002	-21972	64030	107973

Table A-2. Monthly transport rate in m^3/year, south of the inlet.

Month	Positive Q	Negative Q	Net Q	Gross Q
1	14977	-3036	11941	18013
2	7586	-2064	5522	9651
3	5780	-2208	3572	7989
4	2548	-2114	434	4661
5	2222	-1402	820	3624
6	3444	-2525	919	5969
7	4389	-2304	2085	6692
8	3936	-2310	1626	6246
9	7461	-3190	4271	10651
10	10845	-2626	8219	13470
11	13605	-2856	10749	16460
12	13831	-2996	10836	16827

Table A-3. Yearly transport rate in m^3/year, north of the inlet.

Year	Positive Q	Negative Q	Net Q	Gross Q
1974	92384	-68514	23870	160898
1975	107674	-96042	11631	203716
1976	73302	-79843	-6541	153146
1977	90630	-74549	16081	165179
1978	68243	-89886	-21643	158129
1979	101417	-64894	36523	166311
1980	110604	-102483	8121	213088
1981	82459	-98598	-16140	181057

1982	101946	-47983	53963	149929
1983	103758	-102432	1326	206190
1984	94298	-73650	20648	167949
1985	67544	-74779	-7235	142324
1986	77490	-54100	23391	131590
1987	51153	-48255	2898	99408
1988	83500	-58408	25093	141908
1989	65344	-64809	535	130153
1990	120550	-57651	62899	178201
1991	78448	-43557	34890	122005
1992	64505	-52150	12355	116655
1993	34008	-51879	-17871	85888
1994	53670	-63757	-10087	117427
1995	47165	-58436	-11271	105602
1996	39975	-25155	14820	65131
1997	48308	-65267	-16959	113576
1998	90523	-49608	40915	140131
1999	100124	-50259	49865	150382
2000	87599	-52065	35535	139664
2001	45996	-54605	-8609	100600
2002	50575	-41416	9158	91991
2003	30288	-57614	-27325	87902
2004	67278	-52328	14950	119606
2005	60103	-35576	24527	95680
2006	58046	-33155	24890	91201
2007	91875	-99350	-7475	191226
2008	128301	-66769	61532	195071
2009	68370	-54455	13916	122825

Table A-4. Monthly transport rate in m^3/year, north of the inlet.

Month	Positive Q	Negative Q	Net Q	Gross Q
1	12569	-6915	5654	19484
2	6630	-3916	2713	10546
3	4596	-4745	-149	9341

4	2178	-3616	-1438	5795
5	1642	-2861	-1218	4503
6	2205	-5592	-3387	7798
7	2798	-5421	-2623	8219
8	2919	-5111	-2193	8030
9	5987	-6837	-850	12824
10	9699	-5539	4161	15238
11	12455	-6025	6430	18480
12	12362	-6318	6044	18680